

EXTRACTION OF POLYLACTIC ACID DEGRADATION PRODUCTS WITH
SUPERCRITICAL CARBON DIOXIDE

A THESIS SUBMITTED TO
THE GRADUATE SCHOOL OF NATURAL AND APPLIED SCIENCES
OF
MIDDLE EAST TECHNICAL UNIVERSITY

BY

SÜMEYYE KOÇAK BÜTÜNER

IN PARTIAL FULFILLMENT OF THE REQUIREMENTS
FOR
THE DEGREE OF MASTER OF SCIENCE
IN
CHEMICAL ENGINEERING

NOVEMBER 2022

Approval of the thesis:

**EXTRACTION OF POLYLACTIC ACID DEGRADATION PRODUCTS
WITH SUPERCRITICAL CARBON DIOXIDE**

submitted by SÜMEYYE KOÇAK BÜTÜNER in partial fulfillment of the requirements for the degree of **Master of Science in Chemical Engineering, Middle East Technical University** by,

Prof. Dr. Halil Kalıpçılar
Dean, Graduate School of **Natural and Applied Sciences**

Prof. Dr. Pınar Çalık
Head of the Department, **Chemical Engineering**

Assoc. Prof. Dr. Çerağ Dilek Hacıhabiboğlu
Supervisor, **Chemical Engineering, METU**

Prof. Dr. Naime Aslı Sezgi
Co-Supervisor, **Chemical Engineering, METU**

Examining Committee Members:

Prof. Dr. Suna Balcı
Chemical Engineering, Gazi University

Assoc. Prof. Dr. Çerağ Dilek Hacıhabiboğlu
Chemical Engineering, METU

Prof. Dr. Naime Aslı Sezgi
Chemical Engineering, METU

Prof. Dr. Göknur Bayram
Chemical Engineering, METU

Assoc. Prof. Dr. Harun Koku
Chemical Engineering, METU

Date: 25.11.2022

I hereby declare that all information in this document has been obtained and presented in accordance with academic rules and ethical conduct. I also declare that, as required by these rules and conduct, I have fully cited and referenced all material and results that are not original to this work.

Name Last name : Sümeyye Koçak Bütüner

Signature :

ABSTRACT

EXTRACTION OF POLYLACTIC ACID DEGRADATION PRODUCTS WITH SUPERCRITICAL CARBON DIOXIDE

Koçak Bütüner, Sümeyye
Master of Science, Chemical Engineering
Supervisor: Assoc. Prof. Dr. Çerağ Dilek Hacıhabiboğlu
Co-Supervisor: Prof. Dr. Naime Aslı Sezgi

November 2022, 86 pages

Poly(lactic acid) (PLA) is a bio-based polyester derived from starch feedstocks such as sugar cane, sugar beet, or corn. PLA is used in industries like the medical sector, fibers and textiles, packaging, and agriculture. Since the PLA usage area is increasing, its recyclability has gained importance. Currently, chemical recycling for PLA has been conducted by pyrolysis, alcoholysis, or hydrolysis.

In this research, an environmentally benign separation method was developed to recover the PLA depolymerization products. PLA degradation was realized using supercritical carbon dioxide (SCCO₂). Subsequently, degradation products were extracted by SCCO₂. The effects of extraction parameters such as temperature, pressure, and static extraction time on the extracted product distribution and extraction yield were studied.

The effect of temperature was investigated at three different temperatures. Results showed that as extraction temperature increased, extraction yield enhanced since the solubility of decomposition products in SCCO₂ increased. High temperature also

decreased the viscosity of the reaction products, facilitating the mass transfer of the extractable products into the SCCO₂ phase.

The influence of static extraction time was investigated by extending the time. Results revealed extraction yield increased at longer static extraction time since more products could be dissolved in SCCO₂.

The effect of pressure was studied at two different pressures. A slight increase in extraction yield was observed, indicating that increasing the pressure was inadequate to accelerate the mass transfer of the products.

The extracted product composition consisted of D, L lactide, meso lactide, lactic acid, and some unknown products. The highest extraction yield of 89% was obtained at 80 °C, 310 bar for 2 hours of static extraction time. The product obtained in a condenser under these conditions comprised of 53% D, L lactide, 30% meso lactide, 9% lactic acid, and 8% unknown products.

Keywords: Polymer Degradation, PLA, Supercritical Carbon Dioxide, Extraction

ÖZ

POLİLAKTİK ASİT BOZUNMASI SONUCU OLUŞAN ÜRÜNLERİN SÜPERKRİTİK KARBONDİOKSİT İLE ÖZÜTLENMESİ

Koçak Bütüner, Sümeyye
Yüksek Lisans, Kimya Mühendisliği
Tez Yöneticisi: Doç. Dr. Çerağ Dilek Hacıhabiboğlu
Ortak Tez Yöneticisi: Prof. Dr. Naime Aslı Sezgi

Kasım 2022, 86 sayfa

Polilaktik asit (PLA), şeker kamışı, şeker pancarı veya mısır gibi nişasta hammaddelerinden elde edilen biyo bazlı bir polyesterdir. PLA, tıp sektörü, elyaf ve tekstil, paketlenme ve tarım gibi sektörlerde kullanılmaktadır. PLA kullanım alanı arttığı için geri dönüştürülebilirliği önem kazanmıştır. Şu anda, PLA için kimyasal geri dönüşüm piroliz, alkoliz veya hidroliz ile gerçekleştirilmektedir.

Bu araştırmada, PLA bozunma ürünlerini geri kazanmak için çevre dostu bir ayırma yöntemi geliştirilmiştir. PLA bozunması süperkritik karbon dioksit (SCCO₂) kullanılarak gerçekleştirilmiştir. Daha sonra bozunma ürünleri SCCO₂ ile özütlenmiştir. Sıcaklık, basınç ve statik özütlenme süresi gibi özütlenme parametrelerinin özütlenen ürün dağılımı ve özütlenme verimi üzerindeki etkileri incelenmiştir.

Sıcaklığın etkisi üç farklı sıcaklıkta incelenmiştir. Sonuçlar, özütlenme sıcaklığı arttıkça, ayrışma ürünlerinin SCCO₂ içindeki çözünürlüğü arttığı için özütlenme veriminin arttığını göstermektedir. Yüksek sıcaklık aynı zamanda bozunma

ürünlerinin viskozitesini düşürerek özütlenebilir ürünlerin SCCO₂ fazına kütle transferini kolaylaştırmaktadır.

Statik özütleme süresinin etkisi, süre uzatılarak incelenmiştir. Sonuçlar, daha uzun statik özütleme sürelerinde özütleme veriminin arttığını ortaya koymuştur. Bunun nedeni daha fazla ürünün SCCO₂ içinde çözülebilesidir.

Basıncın etkisi iki farklı basınçta incelenmiştir. Özütleme veriminde hafif bir artış gözlenmiştir, bu da ürünlerin kütle transferini hızlandırmak için basıncı artırmanın yetersiz olduğunu göstermiştir.

Özütlenen ürün bileşimi D, L laktit, mezo laktit, laktik asit ve bazı bilinmeyen ürünlerden oluşmuştur. %89 ile en yüksek ekstraksiyon verimi, 2 saatlik statik ekstraksiyon süresi için 80 °C, 310 bar'da elde edilmiştir. Bu koşullar altında yoğunlaştırıcıda elde edilen ürün, %53 D, L laktit, %30 mezo laktit, %9 laktik asit, ve %8 bilinmeyen ürünlerden oluşmuştur.

Anahtar Kelimeler: Polimer Bozunması, PLA, Süperkritik Karbondioksit, Özütleme

To the Founder of Turkish Republic

Mustafa Kemal ATATÜRK...

ACKNOWLEDGMENTS

To begin with, I would like to express my deep gratitude to my supervisor, Assoc. Prof. Dr. erađ Dilek Hacıhabibođlu, for her limitless patience, advice, and encouragement throughout the research. She supported me every time whenever I needed her. I would also like to express my great gratitude to my co-supervisor, Prof. Dr. Naime Aslı Sezgi, for her continuous support, contribution, and criticism during the research. I am very fortunate for conducting my thesis under their guidance and wisdom.

I owe a deep sense of gratitude to my labmates, Seda Sivri, Merve Sarıyer, ađla Bozcuođlu, Salih Ermiř, and Alican Ertas for their friendship, kindness, and support. I must also thank all METU Chemical Engineering Department academic, administrative and technical staff for their help.

I should appreciate my colleagues Gence Bektas, Ahmet Emin Keçeci, Hasan Hüseyin Canar, Hasan Asav, and Bülent Arıkan for their understanding and support. I also would like to express my gratitude to Ayla Kuran and Gökhan Ak for their kind approach and support.

I am thankful to my invaluable friends, Elif Yılmazođlu, Merve Özen Çevik, and Toprak ađlar, for their priceless and genuine friendships during this journey.

Above all, I would like to extend my gratitude to my family. I am glad to thank my father, Yusuf Kenan Koçak, and my mother, Ayře Koçak, for believing in me. I would like to thank my sister, Esra Koçak, and my brothers, Bilal Koçak and Yunus Emre Koçak. They are the joy of my life.

Last but not least, I wish to thank the love of my life, Mehmet Akif Bütüner. Without your patience, persistent encouragement, support, and endless love, I could not have undertaken this journey. You always find a way to cheer me up and comfort me even when I'm most stressed. Thank you for being such an amazing person and being there for me.

TABLE OF CONTENTS

ABSTRACT.....	v
ÖZ	vii
ACKNOWLEDGMENTS	x
TABLE OF CONTENTS.....	xi
LIST OF TABLES	xiii
LIST OF FIGURES	xiv
LIST OF ABBREVIATIONS	xvii
LIST OF SYMBOLS	xviii
CHAPTERS	
1 INTRODUCTION	1
1.1 Polylactic acid.....	2
1.1.1 PLA Manufacturing	2
1.2 Supercritical Fluids	6
1.2.1 Supercritical Carbon Dioxide (SCCO ₂).....	7
1.2.1.1 SCCO ₂ Reaction Medium.....	8
1.2.1.1.1 Polymer Degradation Reactions Using SCCO ₂	10
1.2.2 SCCO ₂ Extraction	12
2 END-OF-LIFE OPTIONS FOR PLA WASTE	17
2.1 Biochemical Degradation.....	18
2.2 Chemical degradation	21

2.2.1	Hydrolysis.....	21
2.2.2	Alcoholysis	24
2.2.3	Pyrolysis	29
2.3	The Aim of the Thesis Study	33
3	EXPERIMENTAL	35
3.1	Materials	35
3.2	Experimental Set-Up	35
3.3	PLA Degradation Reactions Followed by SCCO ₂ Extraction	36
3.4	SCCO ₂ Sweeping Experiments	38
3.5	Concentration determination with GC-Analysis	39
4	RESULTS AND DISCUSSION.....	41
4.1	Repeatability experiments	41
4.2	Effect of Extraction Temperature	48
4.3	Effect of Static Extraction Time	53
4.4	Effect of Extraction Pressure	62
5	CONCLUSIONS	67
6	RECOMMENDATIONS	69
	REFERENCES	71
	APPENDICES	
A.	Solubility Calculations of Lactide in SCCO ₂	81
B.	GC Calibration Factors	83
C.	Equations for Yield Calculation	85

LIST OF TABLES

TABLES

Table 1.1 Materials and microorganisms used for lactic acid production (Madhavan Nampoothiri et al., 2010)	3
Table 1.2 Critical points of the most common fluids (Zhang et al., 2014)	7
Table 1.3 SCCO ₂ extraction examples from the food industry (Wang et al., 2021)	14
Table 3.1 Extraction experiment parameters	38
Table 3.2 GC analysis conditions for prepared products	39
Table A.1 CO ₂ density at given temperature and pressure	81
Table A.2 Lactide mol fraction in CO ₂ and lactide mixture	82
Table A.3 Comparison of lactide mol fraction and required pressure with literature data at given temperature conditions	82
Table B.1 The retention times and response factors of the condensable products.	83
Table B.2 The retention time for unknown products.	84

LIST OF FIGURES

FIGURES

Figure 1.1 PLA manufacturing methods (Auras et al., 2004)	5
Figure 1.2 Commercial process to produce PLA by ROP (Jem & Tan, 2020)	6
Figure 2.1 PLA alcoholysis (McKeown & Jones, 2020).....	24
Figure 3.1 Experimental set-up	36
Figure 4.1 Temperature and pressure profiles of the first (exp1), second (exp2), and third (exp3) repeatability experiments at 40 °C, 310 bar for 60 min static extraction.	42
Figure 4.2 Temperature and pressure profiles of the first sweeping experiments of repeatability experiments at 40 °C, 310 bar for 60 min static extraction.	43
Figure 4.3 Temperature and pressure profiles of the second sweeping experiments of repeatability experiments conducted at 40 °C, 310 bar for 60 min static extraction.	44
Figure 4.4 Gas and solid yields for the repeatability experiments conducted at 310 bar, 40 °C, and for 60 min of static extraction ($T_{rxn}= 220\text{ °C}$, $P_{rxn}=103\text{ bar}$, $t_{rxn}= 30\text{ min}$.).....	45
Figure 4.5 Extraction and reactor yields for the repeatability experiments conducted at 310 bar, 40 °C and for 60 min of static extraction ($T_{rxn}= 220\text{ °C}$, $P_{rxn}=103\text{ bar}$, $t_{rxn}= 30\text{ min}$.).....	46
Figure 4.6 Composition of products for the repeatability experiments conducted at 310 bar, 40 °C and for 60 min of static extraction ($T_{rxn}= 220\text{ °C}$, $P_{rxn}=103\text{ bar}$, $t_{rxn}= 30\text{ min}$.).....	47
Figure 4.7 Temperature and pressure profile of the experiment with the extraction conducted at 60 °C and 310 bar for 60 min of static extraction.	48
Figure 4.8 Temperature and pressure profiles of sweeping experiments conducted at 310 bar, 60 °C for 60 min of static extraction.	49

Figure 4.9 The effects of extraction temperature on the gas and solid yields for the SCCO ₂ extraction conducted at 310 bar and for 60 min of static extraction ($T_{rxn}=220\text{ }^{\circ}\text{C}$, $P_{rxn}=103\text{ bar}$, $t_{rxn}=30\text{ min.}$).....	50
Figure 4.10 The effects of extraction temperature on the extraction and reactor yields for the SCCO ₂ extraction conducted at 310 bar and for 60 min of static extraction ($T_{rxn}=220\text{ }^{\circ}\text{C}$, $P_{rxn}=103\text{ bar}$, $t_{rxn}=30\text{ min.}$).....	51
Figure 4.11 Effect of extraction temperature on product distribution of the extracted products at 310 bar for 60 min of static extraction ($T_{rxn}=220\text{ }^{\circ}\text{C}$, $P_{rxn}=103\text{ bar}$, $t_{rxn}=30\text{ min.}$).....	53
Figure 4.12 Temperature and pressure profile of the experiment with the extraction conducted at 80 °C and 310 bar and for 120 min of static extraction.....	54
Figure 4.13 Temperature and pressure profiles of sweeping experiments conducted at 310 bar, 80 °C for 120 min of static extraction.....	55
Figure 4.14 The effects of static extraction time on the gas and solid yields for the SCCO ₂ extraction conducted at 40 °C and 310 bar ($T_{rxn}=220\text{ }^{\circ}\text{C}$, $P_{rxn}=103\text{ bar}$, $t_{rxn}=30\text{ min.}$).....	56
Figure 4.15 The effects of static extraction time on the gas and solid yields for the SCCO ₂ extraction conducted at 80 °C and 310 bar ($T_{rxn}=220\text{ }^{\circ}\text{C}$, $P_{rxn}=103\text{ bar}$, $t_{rxn}=30\text{ min.}$).....	57
Figure 4.16 The effects of static extraction time on the extraction and reactor yields for the SCCO ₂ extraction conducted at 40 °C and 310 bar ($T_{rxn}=220\text{ }^{\circ}\text{C}$, $P_{rxn}=103\text{ bar}$, $t_{rxn}=30\text{ min.}$).....	58
Figure 4.17 The effects of static extraction time on the extraction and reactor yields for the SCCO ₂ extraction conducted at 80 °C and 310 bar ($T_{rxn}=220\text{ }^{\circ}\text{C}$, $P_{rxn}=103\text{ bar}$, $t_{rxn}=30\text{ min.}$).....	59
Figure 4.18 Effect of static extraction time on product distribution of the extracted products at 40 °C and 310 bar ($T_{rxn}=220\text{ }^{\circ}\text{C}$, $P_{rxn}=103\text{ bar}$, $t_{rxn}=30\text{ min.}$).....	60
Figure 4.19 Effect of static extraction time on product distribution of the extracted products at 80 °C and 310 bar ($T_{rxn}=220\text{ }^{\circ}\text{C}$, $P_{rxn}=103\text{ bar}$, $t_{rxn}=30\text{ min.}$).....	61

Figure 4.20 Temperature and pressure profile of the extraction experiment conducted at 40 °C and 241 bar and for 60 min of static extraction.	62
Figure 4.21 Temperature and pressure profile of sweeping experiments conducted at 40 °C at 241 bar and for 60 min of static extraction.....	63
Figure 4.22 The effects of static extraction time on the gas and solid yields for the SCCO ₂ extraction conducted at 40 °C for 60 min static extraction (T _{rxn} = 220 °C, P _{rxn} =103 bar, t _{rxn} = 30 min.).	64
Figure 4.23 The effects of static extraction time on the extraction and reactor yields for the SCCO ₂ extraction conducted at 40 °C for 60 min static extraction (T _{rxn} = 220 °C, P _{rxn} =103 bar, t _{rxn} = 30 min.).	65
Figure 4.24 Effect of static extraction pressure on product distribution of the extracted products at 40 °C for 60 min of static extraction (T _{rxn} = 220 °C, P _{rxn} =103 bar, t _{rxn} = 30 min.).....	66

LIST OF ABBREVIATIONS

ABBREVIATIONS

FID: Flame Ionization Detector

FTIR: Fourier Transform Infrared Spectroscopy

GC: Gas Chromatography

GCMS: Gas Chromatography-Mass Spectrometry

GPC: Gel Permeation Chromatography

HPLC: High-Performance Liquid Chromatography

IL: Ionic Liquid

PLA: Polylactic acid

ROP: Ring-Opening Polymerization

SCCO₂: Supercritical Carbon dioxide

SCFs: Supercritical Fluids

SFE: Supercritical Fluid Extraction

TGA: Thermogravimetric Analyzer

LIST OF SYMBOLS

SYMBOLS

A_i : Area of species i, mVolts.sec

m_i : mass of species i, mg

n_i : Mol of species i

P : Pressure, bar

P_c : Critical pressure, bar

P_{rxn} : PLA decomposition reaction pressure, bar

RF_i : Response factor of species i

T : Temperature, °C

T_c : Critical temperature, °C

T_{rxn} : PLA decomposition reaction temperature, °C

t_{rxn} : PLA decomposition reaction time, min

$V_{reactor}$: Volume of reactor, ml

W_i : Mass of species i, mg

x_i : Mol fraction of species i

Yield_i: Yield of i, %

GREEK LETTERS

ρ_{CO_2} : Density of CO₂, mol/l

CHAPTER 1

INTRODUCTION

Plastics are one of the most commonly used groups of materials in today's modern world. High production capacity, simple manufacturing techniques, and cost-effective prices contribute to the ubiquitousness of plastics. Their application areas include household goods, packaging, automotive, agriculture, building construction, and electronics since they are light, robust, and stable materials. Recently, plastics' global production has reached almost 368 million tonnes per year (European Bioplastics, 2020). However, as the amount of manufactured plastics increases, plastic waste expands since they are inherently resistant to biodegradation. As a result, it is predicted that almost 32 million tonnes of plastic waste will enter the environment every year (European Bioplastics, 2020).

Such an alarming amount of plastic waste inevitably damages the environment. Environmental destruction caused by plastics is not only limited to the accumulation of plastics in oceans and soil; it is also responsible for the emission of carbon dioxide (CO₂), one of the main greenhouse gas. The plastic production process necessitates both fossil fuels as raw material and energy. Therefore, plastic manufacturing has a significant share of industrial CO₂ emissions. In 2019, the annual emission of CO₂ due to plastic production was reported as 860 million tonnes, which is predicted to attain 2.8 billion tonnes in 2050 (Chemical Sciences and Society Summit, 2020).

These negative impacts of petroleum-based plastics on our planet promoted the biopolymer industry. According to the life cycle assessments, the production of biopolymers requires lower energy compared to the energy required to produce petroleum-based plastics. In addition, biopolymers produce fewer greenhouse gas emissions than conventional plastics (Gironi & Piemonte, 2011). Biopolymers can be specified as a group of polymers that is either bio-based, biodegradable, or both.

They are derived from biomass such as starch, cellulose, fatty acids, sugars, and proteins (Payne et al., 2019). According to market surveys, the production capacity for biopolymers is expected to increase from 2.11 million tonnes in 2020 to 2.87 million tonnes in 2025. Among them, polylactic acid (PLA) has become popular, with a large production capacity of 18.7 % in 2020. This capacity is foreseen to increase to 19.5% in 2025 due to its low environmental impact (European Bioplastics, 2020).

1.1 Polylactic acid

PLA is an aliphatic, biobased, and thermoplastic polyester (Farah et al., 2016). There is growing attention toward PLA due to its mechanical properties, thermal stability, good processability, and low environmental impact (Auras et al., 2004). Therefore, it is considered a perfect replacement for conventional polymers like polystyrene (PS) and polyethylene terephthalate (PET) (Gupta & Kumar, 2007). PLA is used in diverse applications such as biomedical, textile, packaging, service ware, agriculture, and environmental remediation (Castro-Aguirre et al., 2016). PLA is derived from renewable resources such as corn, sugar cane, or sugar beet by the ring-opening polymerization (ROP) route.

1.1.1 PLA Manufacturing

The main monomer of PLA is lactic acid. Lactic acid can be produced by fermentation. The fermentation process is carried out by lactic acid bacteria. The carbon source for the fermentation can be obtained from sugar cane potato, corn cob, tapioca, wheat, or barley (Madhavan Nampoothiri et al., 2010). Lactic acid yield after fermentation differs depending on the used microorganism and fermentation source type. Table 1.1 exhibits different lactic acid yield values obtained from various carbon sources and microorganism types.

Table 1.1 Materials and microorganisms used for lactic acid production (Madhavan Nampoothiri et al., 2010)

Carbon source	Microorganism	Lactic acid yield
Wheat and rice bran	<i>Lactobacillus sp.</i>	129 g/l
Corn cob	<i>Rhizopus sp.MK-96-1196</i>	90 g/l
Cellulose	<i>Lactobacillus coryniformis ssp. torquens</i>	0.89 g/g
Barley	<i>Lactobacillus casei NRRLB-441</i>	0.87–0.98 g/g
Wheat starch	<i>Lactococcus lactis ssp. lactis</i> ATCC 19435	0.77–1 g/g
Whole wheat	<i>Lactococcus lactis and</i> <i>Lactobacillus delbrueckii</i>	0.93–0.95 g/g
Potato starch	<i>Rhizopus oryzae, R. arrhizuso</i>	0.87–0.97 g/g
Corn, rice, wheat starches	<i>Lactobacillus amylovorous</i> ATCC 33620	<0.70 g/g
Corn starch	<i>L. amylovorous NRRL B-4542</i>	0.935 g/g

Lactic acid can also be produced by chemical synthesis. Chemical synthesis of lactic acid proceeds with the hydrolysis of lactonitrile by strong acids (Madhavan Nampoothiri et al., 2010). Other synthesis routes are base-catalyzed degradation of sugars, oxidation of propylene glycol, the reaction of acetaldehyde, carbon monoxide, and water at elevated temperatures and pressures, hydrolysis of chloropropionic acid, and nitric acid oxidation of propylene (Madhavan Nampoothiri et al., 2010). However, chemical synthesis has drawbacks, such as high

manufacturing costs and low lactic acid yield (Datta & Henry, 2006). Therefore, the industry favors lactic acid production by fermentation of carbohydrate sources.

PLA synthesis from lactic acid can be realized by three different methods: direct condensation polymerization, azeotropic dehydration condensation, and polymerization through lactide formation (Auras et al., 2004), as summarized in Figure 1.1. Direct condensation polymerization is considered the cheapest route. However, low molecular weight PLA is obtained through this synthesis route. Therefore, chain coupling agents and adjuvants are necessary to produce PLA with a molecular weight greater than 10^5 Da, increasing the cost and complexity of the process. In the azeotropic solution method, coupling agents and adjuvants are not required. In this approach, the first distillation pressure of lactic acid is reduced for 2 – 3 hours at 130 °C (Auras et al., 2004). Next, most of the condensation water is removed. Following water removal, the catalyst is introduced along with diphenyl ester. Then, a tube packed with 3 Å molecular sieves is attached to the reaction vessel, and the solvent is sent back to the vessel by the molecular sieves for a further 30–40 h at 130 °C. Finally, the high molecular polymer is isolated and precipitated for further purification. Yet, this method is time-consuming, and the addition of catalysts such as boric acid or sulfuric acid can cause undesired degradation and side reactions (Madhavan Nampoothiri et al., 2010).

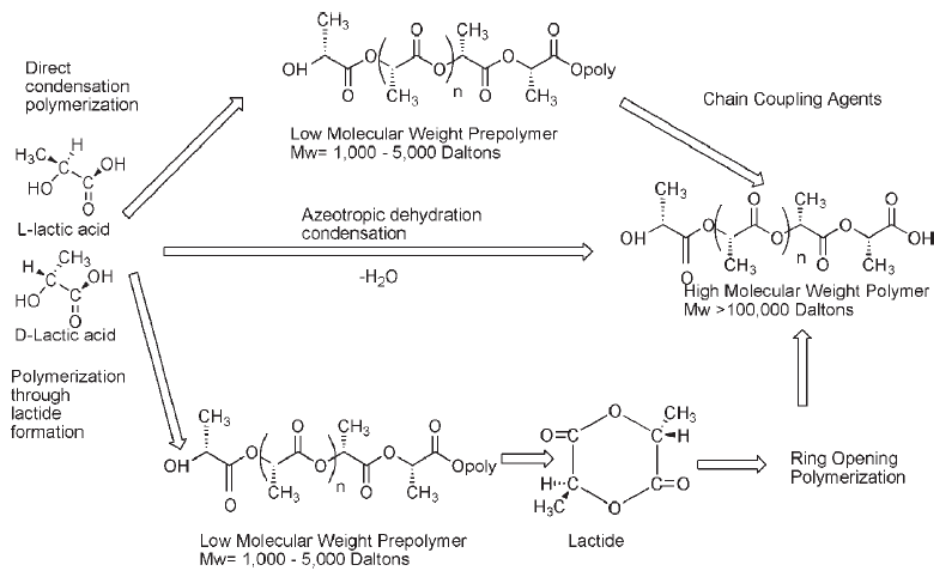


Figure 1.1 PLA manufacturing methods (Auras et al., 2004)

The third method, ring opening polymerization (ROP) or polymerization through lactide formation, is the more efficient approach adopted by the industry (Jem & Tan, 2020). The process of PLA production by ring opening polymerization is seen in Figure 1.2. After fermentation, lactic acid is continuously condensed to produce low molecular weight PLA pre-polymer (Henton et al., 2005). Then, the pre-polymer is transformed into a mixture of lactide stereoisomers using catalysts to improve the rate and selectivity of the intramolecular cyclization reaction. Next, vacuum distillation is then used to purify the lactide mixture. Finally, high molecular weight PLA is synthesized by ROP of lactides. After PLA production, the unreacted monomer is removed and recycled.

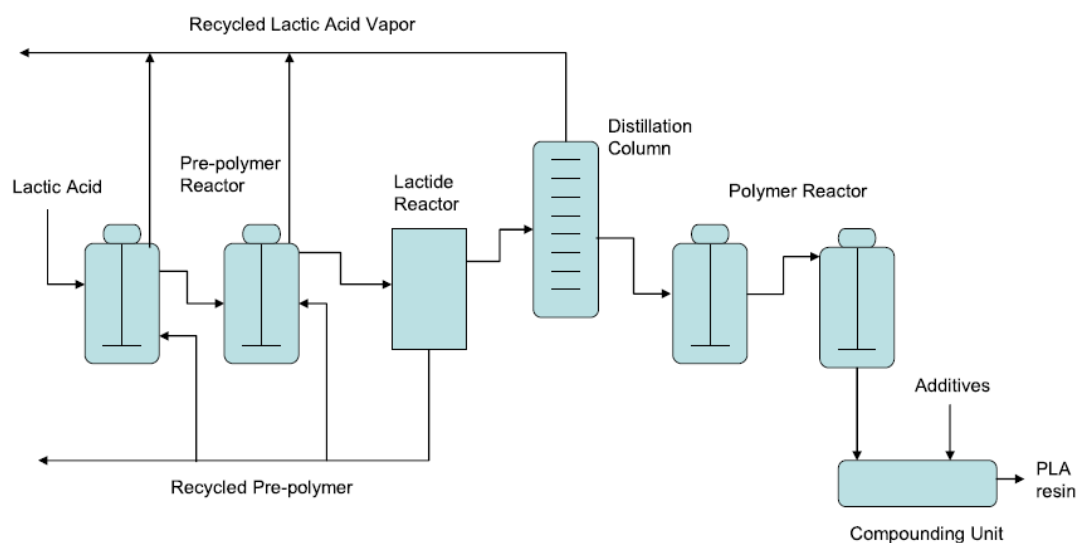


Figure 1.2 Commercial process to produce PLA by ROP (Jem & Tan, 2020)

1.2 Supercritical Fluids

Supercritical fluids (SCFs) are materials at temperature and pressure exceeding the critical temperature and pressure of the material (Knez et al., 2014). SCFs have gas-like viscosity and diffusivity, liquid-like density, and solvation power at supercritical conditions, which makes them perfect solvents for various applications (Knez et al., 2014). The processes utilizing supercritical fluids are environmentally friendly, sustainable, and provide a chance to obtain new products (Knez et al., 2014). They also offer the possibility of separating and drying the product by a simple expansion while the material can be recovered and reused without purification (Knez et al., 2014). Besides, the thermophysical properties of SCFs, such as diffusivity, viscosity, density, or dielectric constants, can be adjusted by changing operation temperature and pressure (Knez et al., 2014). Also, since they have excellent heat transfer properties, they are suggested as a sustainable substitute for the fluids used today in air conditioning and refrigeration systems (Knez et al., 2014). Thanks to their unique properties, SCFs are employed in extracting liquids and solids, polymer processing, supercritical drying and cleaning, refrigeration systems, textile, and chemical reaction media (Knez et al., 2014). Table 1.2 represents the critical points of some

fluids. Among supercritical fluids, supercritical carbon dioxide (SCCO₂) has become remarkable due to its non-toxic nature and mild critical temperature (T_c) and pressure (P_c), 31.1 °C and 73.8 bar, respectively.

Table 1.2 Critical points of the most common fluids (Zhang et al., 2014)

Fluids	T_c (°C)	P_c (bar)
Carbon dioxide	31.1	74
Water	374.1	221
Ethane	32.5	49.1
Propane	96.8	42.6
Methanol	240	79.5
Ethanol	243.1	63.9
Acetone	235	47.6

1.2.1 Supercritical Carbon Dioxide (SCCO₂)

Supercritical carbon dioxide (SCCO₂) is non-toxic, non-flammable, and inert material (Cvjetko Bubalo et al., 2015). Its environmentally benign nature makes it a potential substitution for hazardous and toxic solvents (Cvjetko Bubalo et al., 2015). Besides, since CO₂ used in SCCO₂ processing can be supplied from other industrial processes, additional CO₂ is not generated. (Zhang et al., 2014).

Application areas of SCCO₂ have been expanding due to its favorable properties. Some of them are summarized as follows:

- **Food industry:** decaffeination of coffee and tea; extraction of hops, herbs, spices, antioxidants, and flavors; deoiling of press cakes, etc. (Cvjetko Bubalo et al., 2015)
- **Nutraceuticals and pharmaceuticals:** extraction of carotenoids, lycopene, astaxanthin, sterols, etc. (Cvjetko Bubalo et al., 2015)
- **Cosmetics:** extraction of desired ingredients for cosmeceutical applications and fragrances (Cvjetko Bubalo et al., 2015)
- **Material processing:** microencapsulation, coating, dyeing, crystallization, aerogels, particle formation, impregnation, etc. (Cvjetko Bubalo et al., 2015)
- **Cleaning:** dry cleaning, removal of undesired materials, and cleaning of delicate parts for microelectronic applications, etc. (Knez et al., 2014)
- **Chemical reactions:** polymerization, hydrogenation, catalytic hydrothermal gasification, destruction of toxic organics, enzymatic reactions (Cvjetko Bubalo et al., 2015)

1.2.1.1 SCCO₂ Reaction Medium

Increasing awareness of environmental concerns has modified chemical production in a greener way. Chemical productions are mainly conducted in a reaction medium containing organic solvents, often flammable, toxic, and hazardous. Therefore, potential environmentally benign replacements for these solvents become necessary to develop sustainable processes.

SCCO₂ has also been used as reaction media for chemical synthesis. Its mild critical point, environmentally benign nature, non-toxicity, and non-flammability make SCCO₂ an attractive solvent, although other promising SCFs like water, hydrocarbons, or hydrofluorocarbons are available for chemical reaction medium (Leitner, 2002). There are various following benefits of using SCCO₂ for chemical synthesis;

- **Solvent replacement:** Environmentally friendly nature of SCCO₂ is the initial motivation for replacing organic solvents. No environmental risk is available if accidental contamination of the immediate environment appears with non-toxic and safe CO₂ (Leitner, 2002).
- **Process safety:** Using non-flammable SCCO₂ solvent effectively reduces the risk of explosion in several reaction types, including highly reactive reactants. The outstanding heat transport capacity of SCCO₂ provides effective heat control, preventing hot spots or runaway scenarios in highly exothermic reactions (Leitner, 2002).
- **Improved reaction rates:** Gas-liquid catalyzed chemical reactions are generally diffusion controlled. This controlling step is reduced by eliminating the gas-liquid interface and increasing diffusivity with SCCO₂. Therefore, reaction rates are raised with the reduction in mass transfer barriers (Pereda et al., 2005).
- **Enhancement in porous catalyst activity and product selectivity:** In porous catalysts, activity and product selectivity are influenced by adsorption/desorption and pore transport (Subramaniam, 2001). One of these parameters is generally favorable in conventional gas or liquid reaction medium, while the other is not. To illustrate, the reaction rate limiting step is usually the desorption of heavy hydrocarbons from the catalyst in gas phase reactions, while the limiting step is the transport of reactants/products in the liquid phase reactions (Subramaniam, 2001). Also, achieving the desired fluid properties such as gas-like transport properties, liquid-like solvent power, and heat capacities for optimum system performance is usually problematic with traditional media (Subramaniam, 2001). SCCO₂ eliminates these drawbacks by providing pressure or temperature tunable fluid properties such as diffusivity and viscosity, which are crucial parameters for catalyst activity and product selectivity (Subramaniam, 2001). Besides,

SCCO₂ facilitates the penetration of reactants into the porous structure of the catalyst (Zhang et al., 2014).

- **Catalyst Lifetime and Regeneration:** In some chemical reactions, carbonaceous byproducts, causing catalyst deactivation by coke formation, deposit in the internal and the external surface of the catalyst. SCCO₂ can extract and transport these materials thanks to its high diffusivity, increasing the catalyst lifetime and regenerating the catalyst (Baiker, 1999).
- **Facilitated Separation:** Product separation from classical solvents is usually tedious and energy-intensive. In the SCCO₂ reaction medium, the products are easily separated by simply reducing the pressure of the CO₂ (Baiker, 1999).
- **Process Intensification:** Enhanced reaction rates and easy product separation allow the construction of smaller continuous reactors than conventional continuous reactors for the same performance. This benefit is advantageous in process safety and the space demands of chemical plants (Baiker, 1999).

1.2.1.1.1 Polymer Degradation Reactions Using SCCO₂

SCCO₂ has been used in polymer processing since it is absorbed by polymers and causes a decrease in the viscosity of the polymeric systems due to its plasticizing effect (Knez et al., 2014). The capacity of SCCO₂ to impregnate and plasticize various polymers can make it possible to be used as a reaction medium for polymer recycling (Elmanovich et al., 2020). Besides, since oligomeric and other low molecular weight degradation products are soluble in SCCO₂, the separation of degradation products after or during the procedure is facilitated (Elmanovich et al., 2020).

Polymer degradation in SCCO₂ has recently been an exciting topic for researchers. Elmanovich et al. (2020) investigated the thermal oxidation of polypropylene (PP)

in oxygen-enriched SCCO₂ using a manganese oxide aerogel catalyst at 135 °C. 80 mg of PP and manganese oxide catalyst were placed in high pressure stainless steel reactor with a PP catalyst ratio of 20:1. The reactor was filled with O₂ at ambient temperature with the O₂:PP weight ratio of 1.5:1 and 3:1. Then the vessel was filled with CO₂ at 45 °C until the pressure reached 100 bar. Then, the vessel was placed into a thermostat at 135 °C. After 24 h of exposure, the vessel was decompressed. To compare, the reactor with the same amounts of PP, manganese oxide catalyst, and oxygen, but without SCCO₂, was exposed simultaneously and at the same temperature. After the reaction ended up, 1.5 ml of either deuterated chloroform or tetrahydrofuran was added to the reactor. After 30 min, the obtained solution, containing manganese oxide, was removed from the reactor using a syringe and filtered using a syringe filter. The filtered solution was then analyzed using gas chromatography-mass spectrometry (GCMS). Acetic acid, formic acid, propionic acid, and acetone were detected as the main products. The results revealed that oxidative degradation of PP enhanced under SCCO₂ at lower oxygen content with the main product of acetic acid with 87% yield. The increase in the O₂:PP mass ratio in the presence of manganese oxide increased the selectivity of the oxidation of polypropylene, with acetic acid being the main product.

The same research group examined the thermal oxidation of polyethylene (PE) in pure oxygen and oxygen combined with SCCO₂ at 140 °C (Elmanovich et al., 2022). Thermal oxidation of polyethylene was carried out in O₂-enriched SCCO₂ and pure O₂ under a pressure of 215 and 14 bar, respectively. O₂ to polymer weight ratio was varied with 1:1 and 3:1. PE granules (420 mg for 1:1 O₂:PE weight ratio, 140 mg for 3:1 O₂:PE weight ratio) were placed in a stainless-steel reactor. Then the reactor was sealed and filled with O₂ to a pressure of 10 bar. For each O₂:PE ratio, two types of experiments were performed: in pure oxygen and O₂ enriched SCCO₂. For the latter type, after the reactor was filled with oxygen, it was placed in a thermostat at a temperature of 40 °C, and then, it was connected by a system of capillaries with a CO₂ balloon and pumped with 100 bar of CO₂. Then the reactor was placed in an oven heated to 140 °C for 24 h. The pressure was 14 bar for the experiments in pure

O₂; for the experiments in O₂ enriched CO₂, the pressure was 215 bar. The separation of products from the reactor was not explained in the study. Products of thermal oxidation of PE were analyzed using a thermogravimetric analyzer (TGA), GCMS, and gel permeation chromatography (GPC). TGA demonstrated that the increase in O₂ to PE ratio caused an increase in the volatile fraction of the products from 10 mass % at 1:1 O₂:PE to 40 mass % at 3:1 O₂: PE. GCMS analysis confirmed that acetic acid, formic acid, propionic acid, butyric acid, and valeric acid were volatile products. Acetic acid was the main product among the detected acids. When the process was conducted at a higher O₂:PE ratio, thermal oxidation in pure O₂ gave a higher relative yield of acetic acid with 18% to other detected products than thermal oxidation in O₂ enriched SCCO₂. GPC analysis revealed that SCCO₂ enhances the process of high molecular weight PE decomposition to oligomers at a low O₂:PE mass ratio, further decomposition of oligomers to low molecular weight products undergoes more efficiently in pure oxygen. However, it was shown that if O₂ content was lower, the use of SCCO₂ allowed acceleration of the thermal decomposition of PE into lower molecular weight fractions. Therefore, they concluded that depolymerization under SCCO₂ could be a helpful method for the thermal oxidation of polymeric materials while minimizing oxygen consumption.

1.2.2 SCCO₂ Extraction

Extraction is a separation technique to remove the desired compound from a mixture. Traditionally, extraction is conducted by using organic solvents. Extensive use of these solvents in various industries causes a severe threat to the environment. For this reason, the industry has embraced environmentally friendly extraction technologies (Herrero et al., 2010). The use of supercritical fluids in solute extraction has been expanded since the end of the 1970s (Herrero et al., 2010). The major drawback of supercritical fluid extraction (SFE) is the high investment and operation costs, which lead to more expensive production of extracts than those obtained with conventional extraction methods (Knez et al., 2014). However, this problem is

balanced by avoiding the legal limitations referring to solvent residues in products used for animals or humans (Knez et al., 2014). Furthermore, isolating the products from the total extract and sterilization of the compounds without organic solvent will promote SFE (Knez et al., 2014).

Most supercritical fluid extraction applications adopt carbon dioxide since it has a low cost, environmentally benign nature, and high diffusivity combined with easily tunable solvent strength (Herrero et al., 2010). Besides, the mild critical temperature of SCCO₂ can eliminate problems arising from the thermal decomposition of the solutes (Herrero et al., 2010). Also, once the extraction process is finished, CO₂ removal can be achieved by system depressurization, as CO₂ is a gas under ambient conditions. Thus, solvent-free extracts are produced. This property of CO₂ saves cost and energy for the extraction process since it eliminates the tedious and energy-intensive procedures necessary to remove the solvents (Essien et al., 2020).

SCCO₂ extraction is mainly favored in the food industry. Bioactive compounds can be extracted from the food matrix without affecting the chemical structure of the compounds (Wang et al., 2021). Table 1.3 summarizes the use of SCCO₂ extraction examples from the food industry.

Table 1.3 SCCO₂ extraction examples from the food industry (Wang et al., 2021)

Target Compound	Matrix
Essential Oil	Bergamot seed
	<i>Cymbopogon citronella</i> leaves
	Wild carrot (<i>Daucus carota</i> subsp. <i>maritimus</i>)
Phenolic Compounds	Apple pomace
	Cocoa pod husk
	Citrus peel
Lipids	Roselle seeds
	Palm fruit
	Quinoa seeds
Carotenoids	Sunflower seeds
	Spinach
	Tomato flesh/peels
	Apricot flesh/peels
Alkaloids	Black tea
	Green tea

SCCO₂ extraction technology is not limited to the food industry. It is employed in the pharmaceutical industry for liposomes and biotechnological compounds production, purification of pharmaceutical excipients, sterilization, and enantioselective separation (Herrero et al., 2010). Additionally, the extraction of heavy metals from solid matrices is possible by SCCO₂ extraction. Complexing

agents used in conventional solvent extraction are also applicable in SFE complexation of metal ions as long as they are soluble in SCCO₂ (Herrero et al., 2010). The chemical nature of the complexes determines the solubility of metal complexes in SCCO₂ (Herrero et al., 2010). Various complexing agents such as diisooctyl-thiophosphinic acid (Cyanex 302), sodium diethyldithiocarbamate (Aliquat 336), bis(2-ethylhexyl)phosphoric acid, and bis(2-ethylhexyl)monothiophosphoric acid have been used in SFE of heavy metals (Herrero et al., 2010). Removal of palladium, rhodium, and platinum from automobile catalytic converters; chromium from treated woods; indium, gallium, neodymium, and europium from acidic aqueous solutions are some examples of SCCO₂ extraction applications.

CHAPTER 2

END-OF-LIFE OPTIONS FOR PLA WASTE

Although PLA is a biodegradable polyester, it is resistant to complete microbial degradation under ambient conditions (Farah et al., 2016). Therefore, the waste amount of PLA is expanding rapidly. For this reason, sustainable and effective waste management for PLA has been a substantial issue for researchers.

Conventionally used polymer waste management strategies such as landfilling, incineration, and mechanical recycling are also valid for PLA waste. Landfills are places where disposable waste materials are sent and stored. Although landfilling is the most economical way to manage municipal solid waste, it is less preferred for the disposal of PLA (Castro-Aguirre et al., 2016). Landfills usually do not supply a suitable environment to encourage PLA degradation, so PLA waste continues to accumulate (Castro-Aguirre et al., 2016). As a result, landfilling has some environmental impacts because of gas and leachate formation, health risks, fire and explosions, vegetation damage, unpleasant odors, landfill settlement, groundwater pollution, air pollution, and global warming (Castro-Aguirre et al., 2016). Incineration is a process where waste is combusted for electricity, steam, or heat generation (Castro-Aguirre et al., 2016). The incineration reduces waste volume with energy recovery and minimizes dependency on fossil resources and other fuel sources. PLA waste disposal by incineration saves the energy embedded in PLA. However, since valuable constituents are lost during combustion, incineration does not contribute to the circular economy of PLA. Also, energy saving does not reduce raw material demand for the polymer (Castro-Aguirre et al., 2016). Mechanical recycling involves physical treatments such as shredding, cutting, or grinding the PLA wastes. Mechanical recycling is advantageous since it is comparatively straightforward and cost-effective (Badia & Ribes-Greus, 2016). However, recycled PLA after mechanical treatments generally are used in downgraded applications

since mechanical recycling causes chain scissions and inter/intra – molecular transesterifications, influencing the molar mass distribution and hence mechanical, thermal, and rheological properties of PLA (Badia & Ribes-Greus, 2016). Also, mechanical recycling offers a short-term solution limited to a few cycles (Badia & Ribes-Greus, 2016).

Alternative to traditional PLA waste management, biochemical degradation, and chemical degradation methods are extensively studied in the literature.

2.1 Biochemical Degradation

Biochemical degradation of PLA covers chemical hydrolysis and biodegradation in natural soil microcosm (Qi et al., 2017). A carbon source, microorganisms, and proper environmental conditions such as pH, temperature, and moisture, are required for biodegradation. Biochemical degradation proceeds in two steps, primary degradation and ultimate degradation (Leejarkpai et al., 2011). The polymer chain is split into lower molecular weight PLA oligomers, dimers, etc., in primary degradation due to hydrolysis. Subsequently, produced compounds are taken into microorganisms and decomposed into CO₂, water, or methane by intercellular enzymes (Qi et al., 2017).

In microbial degradation, PLA-degrading microorganisms secrete extracellular depolymerase enzyme for PLA first. Production of extracellular depolymerase enzyme is generally accelerated by supplying inducers such as silk fibroin, gelatin, elastin, some peptides, and amino acids to the microorganisms (Jarerat et al., 2004). Then, depolymerase attack the intramolecular ester bonds of PLA, generating oligomers, dimers, and monomers.

Microorganisms found in soil play an essential role in PLA decomposition. Biochemical degradation of PLA by actinomycetes was studied by Pranamuda et al. (1997) with *Amycolatopsis* HT-32. They demonstrated isolated strain degraded 60% of 100 mg PLA film to lactic acid within 14 days at 30 °C.

Jarerat and Tokiwa studied PLA degradation with *Saccharothrix waywayandensis* (Jarerat & Tokiwa, 2003). 15% of PLA film, whose initial weight was 100 mg, degraded in the basal medium after 7 days. However, they noticed that a 0.1% (w/v) addition of gelatin improved the degrading ability of the microorganism considerably. They reported that 95% of PLA film was degraded to lactic acid after 2 days of cultivation in the presence of gelatin since gelatin stimulates the PLA degrading enzyme production.

The same phenomenon was observed in the degradation of PLA film with 100 mg by *Kibdelosporangium aridum* belonging to the actinomycetes genus. (Jarerat et al., 2003). In a basal medium, PLA weight loss remained only at 24% over 10 days. After introducing 0.1% (w/v) gelatin, 97% of PLA film was degraded to lactic acid% in 14 days.

In addition to actinomycetes, bacterial degradation of PLA was reported by a few researchers. A thermophile, *Geobacillus thermocatenulatus*, isolated from 153 soil samples by the enrichment culture technique showed PLA degrading activity (Tomita et al., 2004). The microorganism was cultivated on 200 mg PLA at 60 °C. After 20 days, the weight of the polymer decreased below 50 mg.

Recently, the biochemical degradation of PLA with M_w of 149243 gmol^{-1} was investigated with *Pseudomonas geniculata* WS3, manure extract, and wastewater sludge extract by introducing different nitrogen sources (Boonluksiri et al., 2021). Biodegradation of PLA was reported in terms of CO_2 production. Degradation was monitored under both submerged and soil burial conditions. This study implemented ammonium sulfate, soytone, sericin, and sodium lactate as nitrogen sources since nitrogen sources enhance the bacterial degradable activity and enzyme production. Results revealed that adding soytone with the combination of *Pseudomonas geniculata* WS3, manure extract, and wastewater sludge extract compared to other nitrogen sources caused more PLA weight loss under submerged conditions. Therefore, experiments for PLA degradation under non-sterile soil burial proceeded

with soytone. The combination of WS3 and soytone induced the highest PLA weight loss of almost 100% to lactic acid within 60 days at 58 °C in the soil environment.

Hajighasemi et al. tested two highly active enzymes, ABO2449 from *Alcanivorax borkumensis* and RPA1511 from *Rhodopseudomonas palustris*, on PLA degradation (Hajighasemi et al., 2016). RPA1511 enzyme provided lactic acid formation from PLA with M_w of $1.0 - 1.8 \times 10^4 \text{ gmol}^{-1}$ and degraded 40% of PLA within 36 hours of incubation at 30 °C. However, enzyme ABO2449 generated less lactic acid during the same incubation time. The addition of 0.1% Plysurf A210G, a type of surfactant used in polymer emulsification, facilitated the binding of enzyme ABO2449 to PLA. Hence, PLA could be degraded by over 90% within two days by the enzyme ABO2449.

There are just a few studies about PLA biochemical degradation by fungal microorganisms in the literature. PLA degrading ability of *Tritirachium album* ATCC 22563 was analyzed in liquid culture at 30 °C for 14 days for PLA with M_n of $2.8 \times 10^5 \text{ gmol}^{-1}$ (Jarerat & Tokiwa, 2001). No significant change in PLA weight loss with pure culture was observed. However, adding 0.1% gelatin to the culture medium increased PLA degradation to lactic acid dramatically since gelatin stimulated enzyme production. 76.4% weight loss in PLA was detected with the addition of gelatin.

Masaki et al. (2005) studied the PLA degrading capacity of a cutinase-like enzyme purified from *Cryptococcus* sp. Strain S-2. After purification, enzymatic degradation of PLA with a molecular weight of 1.4×10^5 was conducted at 30 °C for ten days. The purified enzyme was seen to degrade PLA entirely in 60 hours.

PLA biochemical degradation under composting conditions is faster than in soil. (Muniyasamy et al., 2016). Composting is a biological environment where organic materials are decomposed into carbon dioxide, water, minerals, and humus (Kijchavengkul & Auras, 2008). PLA is reported to degrade under composting conditions after 45 – 60 days at 50 – 60 °C to smaller molecules such as oligomers,

dimers, and monomers (Tokiwa & Calabia, 2006). These small molecules were then metabolized to water and carbon dioxide by microorganisms used in the compost (Tokiwa & Calabia, 2006). Conversely, PLA degradation in soil takes a long time since PLA-degrading microorganisms are scarce in the natural environment compared to other degraders of biodegradable polyesters. Thus, PLA is less vulnerable to microbial attack in the natural environment (Tokiwa & Calabia, 2006).

2.2 Chemical degradation

Chemical degradation is recapturing the monomer from polymer waste or converting it into other functional materials through chemical processes. The conversion of PLA into its monomer has gained significance since obtaining lactic acid from fermentation and separation of lactic acid from the reaction medium is responsible for a prominent part of the PLA production cost (Cristina et al., 2018). In addition, glucose fermentation is more energy-intensive than lactic acid production from the chemical recycling of PLA (Cristina et al., 2018). Thus, chemical recycling is advantageous from an economic and environmental point of view. In the literature, PLA has been chemically depolymerized by hydrolysis, alcoholysis, and pyrolysis.

2.2.1 Hydrolysis

Hydrolysis is a depolymerization method used to convert PLA into its monomer, lactic acid, in an aqueous environment. The hydrolysis reaction rate is highly affected by pH, temperature, molecular weight, and PLA crystallinity (Piemonte et al., 2013). During hydrolysis, water molecules diffuse into amorphous regions of PLA, launching the random chain scission of the ester bonds (Elsawy et al., 2017). Carboxyl groups appear due to the cleavage of the ester bonds, which further catalyzes the hydrolysis reaction (Lamberti, Román-Ramírez, & Wood, 2020). Subsequent degradation of the significant portions of the amorphous regions,

hydrolytic degradation continues from the edge to the center of the crystalline areas. (Elsawy et al., 2017).

Tsuji et al. (2003) examined PLA hydrolysis at elevated temperatures to obtain a high lactic acid yield. Experiments were conducted at temperatures between 180 – 350 °C with 240 mg of PLA. The PLA: water weight ratio was taken as 1:20, and maximum lactic acid yield was achieved at 250 °C with 90% in 10 min. At temperatures higher than 250 °C, racemization and decomposition of lactic acid were detected. Therefore, elevated temperatures were not suggested. The activation energy for hydrolysis reaction between 180 – 350 °C was calculated as 51 kJ/mol.

Piemonte and Gironi (2013) investigated PLA hydrolysis at temperatures of 160 and 180 °C. The pressure for this study was kept at 1.5 MPa. PLA ratio to the water was taken as 1:20 and 1:10 by weight. PLA fragments and distilled water were charged into a batch reactor. To construct kinetic data, the product from the reactor was taken at time intervals of 30 – 150 min. For each time, the liquid product was separated from the reactor, and water was evaporated. Then, the remaining product was centrifuged and filtered to remove solid particles before analysis. The lactic acid formation was confirmed with a Gas chromatograph (GC) equipped with a flame ionization detector (FID). They observed that initial PLA concentration and hydrolysis temperature affected PLA conversion. At 180 °C, after 1 hour of reaction, PLA conversion reached 90% while 5% conversion was obtained at 160 °C for the same reaction time. If the PLA water ratio was 1:20, only 3% conversion was obtained at 160 °C after 1 hour reaction. On the other hand, the conversion increased to 30% when the PLA water ratio was taken as 1:10. They concluded it is possible to obtain concentrated lactic acid solutions by decreasing the water amount; hence energy required to evaporate water decreases. Further investigation for industrial applications was suggested.

Cristina et al. (2018) investigated the kinetic modeling of PLA hydrolysis at temperatures between 170 – 200 °C with reaction time changing from 45 to 90 minutes. PLA: water ratio was taken as 0.11. The products were removed from the

reactor, and filtration was applied after the centrifuge process. Lactic acid and low molecular weight oligomers were reported as hydrolysis products. For product analysis, high-performance liquid chromatography (HPLC) was used. They suggested a kinetic model which describes two hydrolysis steps. The first step was reported as the degradation of PLA with solubilization of oligomers, and the second step was hydrolysis of the oligomers. Complete conversion of PLA was observed at all reaction temperatures (170, 180, 190, and 200 °C). However, 20 min was sufficient to obtain 100% conversion of PLA at 200 °C, while 80 min was required to reach complete conversion at 170 °C.

A suitable catalyst can be exploited to enhance the hydrolysis kinetics of PLA. Song and his colleagues analyzed the hydrolysis of 2 grams of PLA to calcium lactate by using an ionic liquid (IL) catalyst, 1-butyl-3-methylimidazolium acetate ([Bmim][OAc]), for 2 hours reaction (Song et al., 2014). The effect of reaction parameters such as temperature between 120 – 140 °C, ionic liquid dosage, and water amount on hydrolysis was studied. Ionic liquid: PLA weight ratio was changed from 0.1:1 to 0.5:1. Also, the water: PLA molar ratio was altered from 2:1 to 6:1. PLA, water and IL catalyst were charged into the reactor. After 2 hours, the unreacted PLA was separated by filtration and washed using distilled water. The filtrate was titrated by NaOH standard solution. Meanwhile, a given amount of calcium carbonate was added to the obtained filtrate, vigorously agitated and then filtered. The collected filtrate was treated by vacuum distillation for removal of the water to get a mixture of calcium lactate and IL. An equal volume of absolute ethanol was added to the mixture and a white crystalline solid was formed. The resulting mixture was filtered and the cake was dried to obtain calcium lactate. The filtrate was distilled to remove ethanol and IL which was reused directly without further purification. At 130 °C, 93.93% PLA conversion was obtained, while only 27.92% of PLA was converted at 120 °C with 0.5:1 IL PLA ratio and 6:1 water PLA ratio for 2 hours of hydrolysis. Moreover, with an increasing IL: PLA ratio from 0.1:1 to 0.5:1, PLA conversion and calcium lactate yield increased. PLA conversion rose from 43.18% to 93.93% and the yield of calcium lactate increased to 76.08% from 34.98%. Increased water

amount also contributed to the conversion of PLA. When the water amount tripled, the PLA conversion value increased from 83.39% to 93.93%. Furthermore, researchers examined the reusability of ionic liquid as the catalyst. They reported the PLA conversion, and the product yield remained unchanged after the catalyst was used 7 times. They also conducted kinetic studies and found 133.9 kJ/mol activation energy.

2.2.2 Alcoholysis

Alcoholysis is denoted as reactions where alcohol is used as a nucleophile. In this type of reaction, the ester bond cleavage of polyesters by alcohols occurs through a transesterification reaction (Lamberti, Román-Ramírez, & Wood, 2020). PLA can be depolymerized by the alcoholysis method to alkyl lactates as seen in Figure 2.1 (McKeown & Jones, 2020). Alcohol types such as methanol, ethanol, and propanol are used to obtain value-added alkyl lactate products.

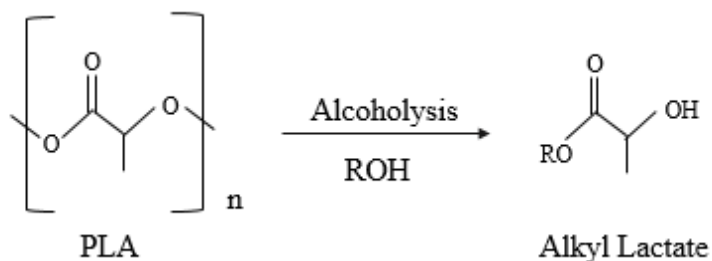


Figure 2.1 PLA alcoholysis (McKeown & Jones, 2020)

Alkyl lactates are green solvents due to their low toxicity and biodegradability (Calvo-Flores et al., 2018). They have several applications in the industry. Ethyl lactate is used in paints, varnishes, gums, dyes, oils, detergents, food additives, cosmetics, and pharmaceuticals (Calvo-Flores et al., 2018). Likewise, propyl lactate is used as a pesticide and food additive, while n-butyl lactate is used in the food industry as an additive and a solvent besides being an ingredient in pharmaceuticals, cosmetics, and paint formulations (Lamberti, Román-Ramírez, McKeown, et al., 2020). Moreover, alkyl lactates can be converted into lactide, contributing to the

circular economy for PLA (Clercq et al., 2018). Sufficient degradation of PLA to alkyl lactates under mild temperature conditions generally requires a proper catalyst (Lamberti, Román-Ramírez, & Wood, 2020).

Alcoholysis of PLA with M_n value of 96000 gmol^{-1} without a catalyst was investigated under microwave irradiation compared to conventional heating (Hirao et al., 2010). The molar ratio of PLA: alcohol was kept constant at 1:10. The reactions were conducted with ethanol at the temperature range of 140 – 180 °C and butanol at 130 – 210 °C. The reaction times were not the same for microwave and conventional heating. Reaction times for alcoholysis experiments with conventional heating were 20 to 60 minutes and that of microwave heating was 2 to 10 minutes. 0.24 g of PLA and alcohol were placed in a Pyrex glass tube and sealed with a silicon cap. The reaction was started when the reaction temperature was reached. The recovery of the products from the reaction environment is not explained. Product identification was investigated based on the optical purity of the products, and it was accomplished via HPLC. Gel permeation chromatography (GPC) results revealed that during alcoholysis, the molecular weight of PLA decreased for both alcohol type and heating methods to 8200 gmol^{-1} . Activation energies were calculated based on the change in molecular weight for different temperatures. 113.1 kJ/mol was obtained in ethanol alcoholysis for two heating techniques. Conversely, for alcoholysis by butanol between 130 – 170 °C, activation energies of 50.2 kJ/mol and 58.6 kJ/mol were observed for microwave and conventional heating. However, activation energies of 104.7 kJ/mol for microwave heating and 108.9 kJ/mol for conventional heating were detected for the temperature range of 170 – 210 °C. They highlighted the alcoholysis mechanism was evaluated to be the same for both heating methods, but microwave heating enhanced the reaction kinetics.

A different catalyst, ferric chloride (FeCl_3), was also implemented in the methanolysis of PLA which has M_w of 225000 gmol^{-1} (H. Liu et al., 2015). They investigated the effect of reaction conditions on the methanolysis of PLA using ferric chloride (FeCl_3) catalyst. The reaction was conducted at temperatures between 100

– 140 °C, and the reaction time was changed from 1 to 4 hours. PLA molar ratio to the methanol was altered between 1:1 to 1:6, and similarly, the molar ratio of catalyst to PLA was taken between 0.005:1 to 0.03:1. After the reaction was finished the undepolymerized PLA was removed by filtration, the residual PLA was collected. Simultaneously, the filtrate was distilled to recover unreacted methanol at atmospheric pressure and the main product (methyl lactate) at reduced pressure. The remaining part after distillation was mainly FeCl₃, which was reused directly as a catalyst without any treatment. Under optimum conditions of methanol: PLA=5:1, catalyst: PLA=0.01:1, 130 °C, and 4 hours, 96% of PLA conversion and 87.2% methyl lactate yield were achieved. After the catalyst was removed from the reaction medium, it was used again to discover its reusability. The PLA conversion and methyl lactate yield were preserved even after using the catalyst six times. Kinetic analysis was also conducted for the reaction system, and the activation energy between the 110 – 135 °C range was found to be 32.41 kJ/mol.

Ionic liquids were also implemented as a catalyst for PLA degradation. Song et al. (2013) tested the performance of several ionic liquids, 1-Butyl-3-methylimidazolium chloride ([Bmim][Cl]), 1-Butyl-3-methylimidazolium hexafluorophosphate ([Bmim][PF₆]), 1-Butyl-3-methylimidazolium acetate ([Bmim][Ac]), and 1-Butyl-3-methylimidazolium hydrogen sulfate ([Bmim][HSO₄]) in PLA methanolysis reactions with PLA pellets ($M_w = 400000 \text{ g mol}^{-1}$). The effect of ionic liquid amount, reaction time, reaction temperature, and methanol dosage on PLA conversion and methyl lactate yield were examined. The temperature was changed from 90 to 120 °C. The employed weight ratios of methanol to PLA were 4:1, 5:1, and 6:1; the weight ratios of catalyst to PLA were 0.01:1, 0.02:1, 0.05:1, and 0.10:1. The reaction time was kept constant at 3 hours. When the reaction was completed, undepolymerized PLA was separated by filtration. The residual PLA was collected, dried, and weighed. Simultaneously, the filtrate was distilled to recover unreacted methanol at atmospheric pressure and obtain the product methyl lactate by vacuum distillation. The products were identified by GPC. Among used ionic liquids, [Bmim][Ac] showed the highest catalytic performance. High PLA conversion

(96.8%) and methyl lactate yield (91%) were obtained at 115 °C for 3 hours when the molar ratio of methanol to PLA and weight ratio of [Bmim][Ac] to PLA was equal to 6:1 and 0.02:1, respectively. It was shown that [Bmim][Ac] could be used up to 6 times with an insignificant decrease in PLA conversion and product yield. The activation energy for the methanolysis reaction was also detected as 38.3 kJ/mol.

A similar study was conducted with acidic functionalized ionic liquids (1-butyl-3-methylimidazolium tetrafluoroborate ([Bmim][BF₄]), 1-methylimidazolium hydrogensulfate [Mim][HSO₄], pyridinium hydrogen sulfate ([HSO₃-pPydin][HSO₄]), and 1-methyl-3-(3-sulfopropyl)-imidazolium hydrogen sulfate ([HSO₃-pmim][HSO₄])) as catalysts for PLA methanolysis (Song et al., 2014). The M_w of PLA pellets for the degradation reaction was 38000 gmol⁻¹. PLA (2 g), methanol, and IL were charged to the reactor with methanol PLA molar ratio of 5:1, and IL PLA weight ratio of 0.02:1. The reaction temperature was 115 °C for 3 hours reaction. After the reaction ended, undepolymerized PLA was removed by filtration. The residual PLA was collected, dried, and weighed. Meanwhile, the filtrate was distilled to recover the unreacted methanol at atmospheric pressure and obtained the main product (methyl lactate) was removed by vacuum distillation. Product identification was done by FTIR. Among ionic liquids, ([HSO₃-pmim][HSO₄]) showed higher catalytic performance with 94.8% PLA conversion and 86.9% methyl lactate yield. Therefore, optimization experiments were completed using [HSO₃-pmim][HSO₄]. For optimization reaction experiments, the temperature was changed from 95 to 120 °C, and the reaction time was altered between 2 – 4 hours. The effect of methanol and catalyst dosage was also investigated. The mole ratio of methanol to PLA was studied between 2:1 – 6:1. Similarly, the weight ratio of IL to PLA was taken in the range of 0.005:1 – 0.03:1. 97% PLA conversion and 88.7% methyl lactate yield were obtained under 115 °C for 3.5 hours, with that a weight ratio of IL: PLA was 0.02:1 and a molar ratio of PLA: methanol was 1:5. Similar to the previous study, it was demonstrated that the ionic liquid could be used up to 6 times. The activation energy for the methanolysis reaction was found as 47.01 kJ/mol.

Another type of IL, butylmethylimidazolium tetrachloroferrate ([Bmim][FeCl₄]), was also used to catalyze methanolysis of PLA with M_w of 220500 g mol^{-1} (H. Liu et al., 2017). The reaction temperature was altered from 100 to 120 °C while the reaction time was changed between 2 – 3 hours. The molar ratio of methanol to PLA was selected as 3:1, 5:1, and 7:1, while the molar ratio of IL to PLA was kept as 0.0010:1, 0.0020, and 0.0025:1. PLA, methanol, and IL were charged to the reactor. When the reaction finished, the unreacted methanol was recovered by atmospheric distillation and the product (methyl lactate) was collected by vacuum distillation. Product identification was completed via FTIR. Under optimized conditions, which were methanol PLA molar ratio of 5:1, IL PLA molar ratio of 0.0025:1 for 3 hours reaction at 120 °C. 99.3% PLA conversion and 94.6% methyl lactate yield were obtained under optimized conditions. The activation energy for the methanolysis reaction was found as 21.28 kJ/mol. Moreover, the ionic liquid catalyst was reusable up to 6 times.

A different research group used DBU-based ionic liquids to catalyze PLA degradation (Liu et al., 2019). In this study, researchers synthesized the DBU-based ionic liquid by using acetic acid ([HDBU][AA]) as the anion. Typically, 2 g PLA was charged into the reactor with methanol and IL. The reaction temperature range was 90 – 120 °C, reaction times were in between 2 – 7 hours. The molar ratio of methanol to PLA was in the range of 1:1 – 9:1, and the molar ratio of IL to PLA was changed from 0.015:1 to 0.075:1. After the reaction ended up, the unreacted PLA was collected by filtration, washed with methanol and dried under vacuum. The filtrate was distilled under a vacuum to remove the methanol and collected the methyl lactate. Product characterization was done by using Fourier transform infrared spectroscopy (FTIR). A complete conversion of PLA with 91% methyl lactate yield was achieved using [HDBU][AA] with the molar ratio of methanol to PLA 5:1, IL PLA molar ratio of 0.02:1 at 100 °C for 5 hours of reaction. The durability of the catalyst was also examined. FTIR results indicated that even after 6 runs, the characteristic peaks of the ionic liquid were retained.

2.2.3 Pyrolysis

Pyrolysis, also known as thermolysis, refers to the chemical degradation of organic materials under heat (Qureshi et al., 2020). It is one of the vital degradation techniques for degrading various polymeric materials into valuable fuel oil or monomers. Many traditional polymers, including PE, PP, PMMA, PET, PS, PVC, etc., have been converted into beneficial products using the pyrolysis method (Qureshi et al., 2020).

PLA is synthesized by the ring-opening polymerization of lactides. Since the concentration of lactide in the reversible ring-opening polymerization reaction depends on the temperature, the lactides can be reformed through the pyrolysis of PLA (Nishida, 2010). However, the pyrolysis mechanism of PLA has complex nature. In addition to lactide, volatile compounds come out. There are several studies focused on PLA pyrolysis.

Mcneill and Leiper studied 2.5 mg PLA degradation under controlled heating at a rate of 10 °C/min and isothermal conditions using a thermogravimetric analyzer (TGA) (Mcneill & Leiper, 1985b)(Mcneill & Leiper, 1985a). It was shown that under the controlled heating program, PLA broke down in a single step between 250 and 450 °C. The main products were cyclic oligomers, lactide, carbon dioxide, and acetaldehyde. In the isothermal experiments (230, 277, 322, 362, and 440 °C), product distributions changed with different temperatures. FTIR spectroscopy revealed that oligomers, lactide, carbon monoxide, and acetaldehyde were observed for all temperatures. At 230 °C, oligomers, lactide, and acetaldehyde formed. However, carbon dioxide and methyl ketene formation was observed at higher temperatures. Also, it was reported that the main thermal degradation mechanism was due to unzipping depolymerization, caused by back-biting reactions, of hydroxyl end groups of PLA. For this reason, acetylation of hydroxyl end groups contributed to thermal stabilisation of the polymer. The researchers calculated activation energy as 119 kJ/mol between 240 – 170 °C by using first order kinetics.

Noda and Okuyama (1999) implemented aluminum, tin, zinc, and zirconia metals and their compounds, including metal alkoxides, organic acids, enolate salts, halides, and oxides, as intramolecular transesterification catalysts for PLA ($M_n = 99800 \text{ gmol}^{-1}$). PLA and the catalyst mixture with two different catalyst PLA molar ratios (0.2:1 and 1:1) were heated to 190 – 245 °C and distilled under 4 – 5 mmHg. The distillate was analyzed via GC. L – lactide, meso – lactide, and D – lactide were reported as the products. From the catalytic performance of view, tin gave the best result in terms of lactide production with 89% yield for 1 hour. The performances of the catalysts were compared with that of the Sn compound.

Nishida et al. also concentrated on the effect of tin content on thermal PLLA degradation (Nishida et al., 2003). They prepared PLLA film samples containing different Sn concentrations (20 – 607 ppm) with different molecular weights ($121300 - 158000 \text{ gmol}^{-1}$). They performed dynamic pyrolysis using TGA for 8 mg PLLA film samples from room temperature to 400 °C. Isothermal pyrolysis reactions were conducted in a glass tube oven with 200 mg of PLLA film samples. The temperature of the oven was increased gradually to 350 °C and kept at this temperature for 20 minutes. Pyrolysis products were detected by pyrolysis-gas chromatography/mass spectrometry (Py-GC/MS). Results of isothermal pyrolysis revealed that pyrolysis of PLLA with high tin content resulted in lactide production, whereas cyclic oligomers formed from PLLA films with low tin content. In dynamic pyrolysis experiments, they demonstrated that as the tin content of PLLA increased, the degradation started at lower temperatures, and activation energy decreased.

Zou et al. conducted a similar study (Zou et al., 2009). The thermal decomposition of the 10 mg PLA sample ($M_w = 69000 \text{ gmol}^{-1}$) at different heating rates (5, 10, 20, 30, 40 °C/min) is analyzed by thermogravimetry coupled to Fourier transform infrared spectroscopy. The results demonstrated that the onset temperature increased as the heating rate increased. Averagely, PLA decomposition started around 275 °C, and complete depolymerization was observed at around 420 °C. The shift of onset temperature with a higher heating rate was because of the shorter time required for a

sample to reach a given temperature at the higher heating rates. Gaseous products of cyclic oligomers, lactide, acetaldehyde, carbon monoxide, and carbon dioxide were detected. While carbon monoxide progressively decreased, acetaldehyde and carbon dioxide existed until the end of the degradation. They also analyzed the degradation kinetics by three different methods. The activation energies for PLA pyrolysis were 177.5 kJ/mol, 183.6 kJ/mol, and 181.1 kJ/mol by applying the Ozawa-Flynn-Wall method, Friedman's method, and Kissinger's method, respectively.

In another study, the catalytic behavior of magnesium oxide (MgO) and calcium oxide (CaO) in the thermal depolymerization of PLA was studied (Fan et al., 2004). PLA was blended with CaO and MgO to obtain PLA/metal oxide composites. The experiments were conducted with a composite of metal oxide and PLA. TGA was conducted using 5 mg of PLA film sample. Two heating programs were employed for the pyrolysis of PLLA, dynamic heating and isothermal heating. In the dynamic heating process, heating rates of 1, 3, 5, 7, and 9 K min⁻¹ were applied from room temperature to 400 °C. In the isothermal heating process, the sample was heated from 60 to 250 °C at a heating rate of 20 °C min⁻¹ and kept at 250 °C for 10 min. Product analysis was completed with GC. Dynamic heating results showed that both catalysts lowered the degradation temperature scale. The degradation temperature for purified PLA was reported as 270 °C. Conversely, PLA/CaO composite started to degrade at 180 °C while the initial degradation temperature of PLA/MgO composite was 210 °C. From both PLA composite films, 98% of the obtained products consisted of lactides rather than cyclic oligomers generated through the pyrolysis of purified PLA. Although CaO lowered the degradation temperature, it induced racemization problems below 250 °C. However, racemization was barely observed in PLA/MgO composite at temperatures lower than 250 °C. This outcome was attributed to the lower basicity of the MgO compound. They also reported activation energies for PLA pyrolysis reactions. They found that the activation energy increased from 147 kJ/mol to 160 kJ/mol, then decreased to 125 kJ/mol towards the end of the pyrolysis for pyrolysis conducted with CaO. Yet, the PLA/MgO composite activation energy remained at 120 – 130 kJ/mol.

Wang et al. (2019) examined the catalytic effect of nanosized zinc oxide (ZnO) and titanium oxide (TiO₂) on the thermal degradation of PLA. The melt blending method combined PLA and metal oxides to prepare hybrid materials. 8 mg of PLA hybrid sample was loaded and heated from room temperature to 750 K in non-isothermal mode. Both metal oxides allowed PLA to degrade at a lower temperature than pure PLA. The thermal stability of PLA has considerably decreased by more than 85 K by filling nanosized ZnO and slightly decreased between 2 and 10 K by adding TiO₂ nanoparticles. It was concluded that ZnO exhibited a stronger catalytic effect than TiO₂. In addition, compared with pure PLA, the activation energy was decreased by 11 to 32 kJ/mol for the PLA/TiO₂ hybrid and 35 to 59 kJ/mol for the PLA/ ZnO hybrid.

Lately, thermal depolymerization of PLA was performed with aluminum-loaded silica aerogels using TGA (Sivri et al., 2019). Catalysts were prepared by loading 2.5, 10, and 15 wt% metal, and their structure was understood to be mesoporous by the BET method. The surface areas of the samples changed from 743 m²/g to 510 m²/g with the increasing aluminum amount. Since the acidity of the catalyst plays a vital role in PLA degradation, the total acidic capacity of the catalysts was measured by temperature-programmed desorption (NH₃-TPD). As aluminum content was boosted, the acidity of the synthesized particles increased. In the thermal PLA degradation experiment, it was displayed that an increase in alumina amount on the silica aerogel rendered degradation to be realized at lower temperatures. The activation energy from PLA degradation without a catalyst was 262 kJ/mol. The use of silica aerogel with 15 wt% aluminum loading reduced the activation energy to 190 kJ/mol.

In addition to the chemical degradation methods mentioned above, PLA depolymerization into its monomers using SCCO₂ was patented (Sivri et al., 2020). Other than this patent document, no study is available in the literature on the degradation of PLA in SCCO₂. In this study, PLA degraded under SCCO₂ without any organic solvent, water, or catalyst. Lactide isomers with 94% purity were obtained from the degradation of PLA under SCCO₂.

2.3 The Aim of the Thesis Study

An increase in demand for PLA in various industries will cause PLA pollution since PLA is not readily degradable in the natural environment. For this reason, some PLA waste management strategies have been suggested.

In landfilling, PLA wastes are accumulated and buried in landfills. This method does not serve as a sustainable solution since many problems such as gas and leachate formation, air pollution, groundwater pollution, and explosions, arise. Also, valuable monomers in PLA structures are not recovered in landfilling. The incineration of PLA wastes is another waste management strategy. The energy embedded in the PLA chain can be retrieved by burning it. However, again, PLA monomers are lost in this method. Mechanical recycling of PLA wastes is a cost-effective method, but it is limited to a few cycles, and deterioration in the mechanical properties of PLA is observed. PLA degradation by microorganisms has been continuing. The major drawbacks of this method are that the PLA degraders are limited and not found in every soil type.

Therefore chemical degradation methods, which are hydrolysis and alcoholysis, come forward to obtain monomeric compounds from PLA with high efficiencies. Yet, these methods employ water and organic solvents, which is inconsistent with sustainable process design principles. Also, the recovery of the products and the catalysts from the reaction medium contains a tedious separation workload and energy-intensive process.

This thesis study aims to degrade PLA to its monomers and separate these monomers from the reactor without using any organic solvent or water. In this regard, a supercritical fluid extraction process is developed for the first time to isolate the monomers and other products of PLA degradation, which can be dissolved in SCCO₂. In other words, environmentally benign separation of the PLA degradation products is the objective of the thesis study.

CHAPTER 3

EXPERIMENTAL

3.1 Materials

PLA used in the experiments was supplied from NatureWorks-2003D and had the following properties: specific gravity: 1.24, melt flow rate: 6 g/10 min, melting point: 145–160 °C. Carbon dioxide (CO₂) (99.9% purity) and acetone (99.9% purity) were provided from Linde Gas (Turkey) and Sigma Aldrich, respectively.

3.2 Experimental Set-Up

PLA degradation and subsequent extraction experiments are conducted in a well-sealed stainless steel high-pressure reactor (Micro Reactor model 4592, PARR Instruments, USA) with a heating jacket seen in Figure 3.1. The vessel is coupled with a pressure transducer, thermocouple (OMEGA, KMQXLIM150U-150 OR K type), and reactor controller (Model 4848, PARR Instruments, USA) to monitor the pressure and control the temperature. Pressurized CO₂ is supplied to the reactor by a syringe pump (Model 260D, Teledyne ISCO, USA) connected to the inlet valve of the reactor. The temperature of the pump is adjusted by a water circulator. The exit path, including the reactor outlet valve and the discharge line, is covered with a heating tape coupled with a thermocouple and a controller to prevent products from freezing and accumulating in this part during extraction. The discharge line is connected to the glass jars in a container filled with ice cubes and water to provide precipitation of the products into the jars.

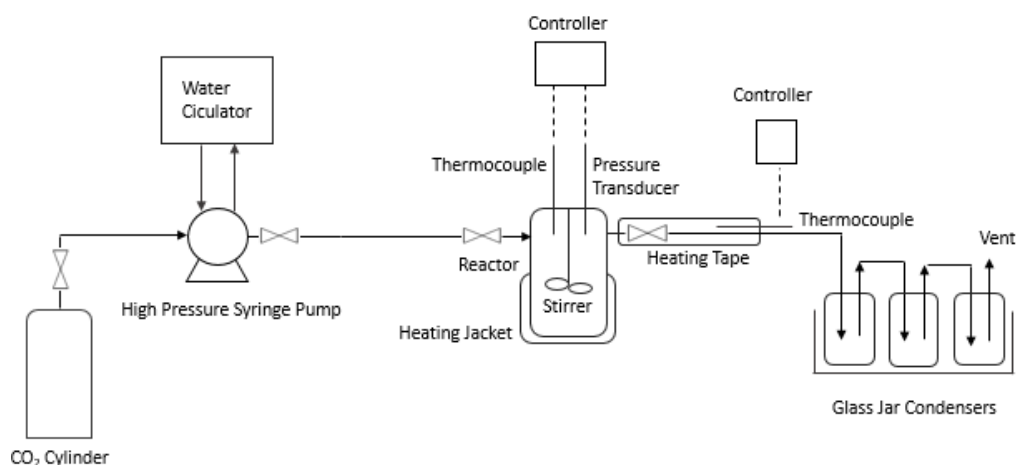


Figure 3.1 Experimental set-up

3.3 PLA Degradation Reactions Followed by SCCO₂ Extraction

Initially, 1 g of PLA is introduced into the high-pressure reactor. The reactor is sealed, and the syringe pump is connected to the reactor. CO₂ is introduced to the reactor along with the heating of the reactor incrementally till the reactor temperature and pressure reach 220 °C and 103 bar. These conditions are the depolymerization reaction conditions and are above the T_c and P_c of CO₂ which are 31.1 °C and 74 bar, respectively. The reaction time is started under these conditions, while the reaction medium is stirred at 70 rpm. After 30 minutes, the reaction is completed, and the heating jacket is separated to allow the reactor to cool down to the extraction temperature. Meanwhile, the pressure of the syringe pump is adjusted to the extraction pressure while the temperature of the syringe pump is kept at 40 °C for all extraction experiments. When the reactor temperature decreases to the extraction temperature, the vessel is slowly pressurized to the extraction pressure. After reaching extraction conditions, static extraction of the product by SCCO₂ starts and continues for a specified extraction time. Before the dynamic extraction begins, the temperature of the heating tape is increased to 114 °C, which is above the melting point of the products obtained after the PLA decomposition reaction. The pressure

in the reactor increases with the effect of temperature increase in the outlet valve due to the heating tape. For this reason, the syringe pump pressure is adjusted to be more than the last read pressure of the reactor to prevent back pressure. As soon as the static extraction part is finished, the inlet and outlet valves of the vessel are opened to provide continuous SCCO₂ flow for the dynamic extraction part. The flow rate of SCCO₂ is kept constant by adjusting the opening of the outlet valve. During dynamic extraction, extracted products precipitate into glass jars (or condensers) since the state of CO₂ changes from supercritical to the gas phase when it is opened to the atmospheric conditions. Therefore, the product is easily separated from CO₂. For this study, the extraction behavior of SCCO₂ is investigated based on parameters such as pressure, temperature, and time. The extraction parameters are given in Table 3.1. The extraction temperature and pressure ranges are selected based on the solubility studies of lactide and lactic acid, which are expected to be the major depolymerization products, in supercritical carbon dioxide (Gregorowicz, 2008), (Gregorowicz, 1999). The related solubility calculations for the parameter selection are given in Appendix A. All the temperature and pressure conditions for the extraction are above the T_c and P_c of SCCO₂. In the experiments, heating, and pressurization of the reactor take a long time. Thus, conditions of PLA decomposition reactions should be selected to complete the experiments in 10–12 hours. Based on the experience of our research group, the shortest decomposition reaction conditions, 220 °C, 103 bar, and 30 min, were chosen. The repeatability and reliability of the decomposition reaction followed by extraction and subsequent sweeping experiments were determined by repeating the experiments three times. The standard deviation of 3.1 wt.% was found for the extraction yield from the repeatability experiments.

Table 3.1 Extraction experiment parameters

Parameters	
Pressure (bar)	241
	310
Temperature (°C)	40
	60
	80
Time (min)	60
	120

3.4 SCCO₂ Sweeping Experiments

The products obtained from the degradation of PLA under SCCO₂ are not entirely removed from the discharge line and locations close to the discharge line of the reactor. Therefore, SCCO₂ sweeping experiments are required to clean the discharge line before the next experiment and to collect the degradation products in that line. Sweeping experiments include only static extraction and dynamic extraction. The extraction parameters are similar to the SCCO₂ extraction after the PLA degradation reaction. For the sweeping experiments, the empty reactor is sealed and heated to the extraction temperature. After the desired extraction temperature is attained, the reactor is pressurized to the extraction pressure by the ISCO pump. Next, static extraction starts and continues for the determined extraction time. As soon as the static extraction finishes, the inlet and outlet valves are opened, and the dynamic extraction part begins with the continuous CO₂ flow. The products in the discharge line and other reactor parts precipitate into the glass jars. After the sweeping experiment finishes, the amount of products in the jars and the products that appeared in the reactor are weighted. Two sweeping experiments are applied after PLA decomposition followed by extraction experiments. The obtained products in the

glass jars and reactor are dissolved in the acetone. Then, the prepared samples are analyzed using GC with the same analysis conditions in Table 3.2. The repeatability of the experiments is verified with the extraction experiments repeated three times, which were carried out at 40 °C, 310 bar, and for 60 min of static extraction.

3.5 Concentration determination with GC-Analysis

The degradation products obtained without SCCO₂ extraction, the products collected in precipitation jars with SCCO₂ extraction, and the products remaining in the reactor after SCCO₂ extraction are dissolved in acetone. The prepared product solutions are analyzed using Varian CP 3800GC equipped with a TRB-1 capillary column and flame ionization detector (FID). The analysis conditions are given in Table 3.2.

Table 3.2 GC analysis conditions for prepared products

Injection amount	0.1 µL
Column flow	0.3 mL/min
Detector temperature	275 °C
Column pressure	5 psi
Analysis time	45 min
Carrier gas	He
Split ratio	100

CHAPTER 4

RESULTS AND DISCUSSION

Before the SCCO₂ extraction experiments, PLA degradation under SCCO₂ is conducted under 220 °C, 103 bar for 30 minutes. With the decomposition reactions, PLA is converted into gas and a highly viscous fluid product, which is referred to as solid. According to the results, 30% of the depolymerized PLA leaves the reactor as gas products, while the remaining 70% stays in the reactor and is referred to as solid products. In other words, 30% gas yield and 70% solid yield are obtained from depolymerization experiments. The main gas product was determined as acetaldehyde by our research group. PLA mainly decomposes to meso lactide, D, L lactide, and lactic acid, which are solid products. The mechanism of the decomposition reaction is under investigation by our research group. These products are analyzed using GC, and the number of moles was calculated using the response factors and the related equation, which are given in Appendix B. The products are intended to be extracted from the reactor with SCCO₂ under various extraction conditions. In the extraction experiments, the flow rate for the dynamic extraction part of the experiments is kept at 4.5 (\pm 0.3) mL/min. In addition, coke formation in the solid part between 10 – 15% is observed. Therefore, the amount of coke is taken into consideration when extraction yield is calculated. The yield equations of the solid, gas, extraction, and left in the reactor are given in Appendix C.

4.1 Repeatability experiments

Three sets of experiments that employ extraction parameters of 310 bar, 40 °C, and 60 min static extraction are conducted to detect the repeatability of the experiments. Temperature (T) and pressure (P) profiles of the repeatability experiments are demonstrated in Figure 4.1. For each experiment, two sweeping experiments are

conducted. The first and second sweeping experiment profiles are given in Figure 4.2 and Figure 4.3, respectively.

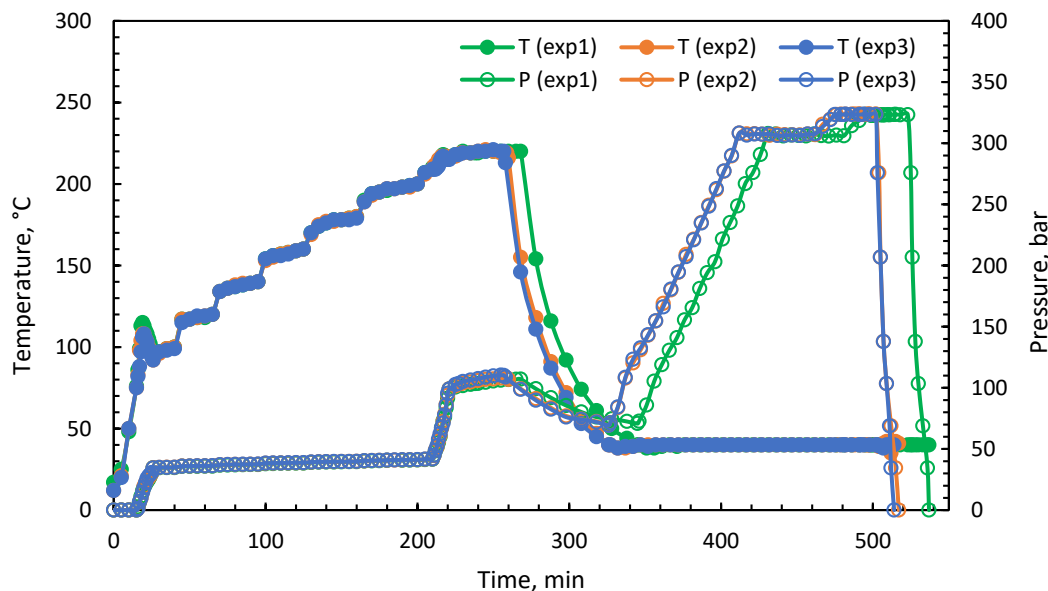


Figure 4.1 Temperature and pressure profiles of the first (exp1), second (exp2), and third (exp3) repeatability experiments at 40 °C, 310 bar for 60 min static extraction.

As seen in Figure 4.1, The reactor temperature and pressure reach reaction conditions at 240 min while there are PLA pellets in the reactor. The reactor temperature is kept constant at 220 °C for 30 min. Meanwhile, a slight increase in pressure is observed since the formation of gas products increases the reactor pressure. After 30 minutes, the reaction is finished, and the reactor is cooled down to 40 °C in 80 minutes. Due to the effect of cooling, a decrease in reactor pressure is observed. When the reactor temperature reaches 40 °C, the reactor is pressurized to extraction pressure, 310 bar, and the temperature is kept at 40 °C. Pressurization of the reactor to the extraction pressure takes 85 minutes. In the pressure plot, the first plateau observed after the pressurization of the reactor corresponds to the static extraction part of the experiment. Static extraction continues for 60 minutes. The slight pressure increase observed at the end of the static extraction part is due to the pressure of the syringe pump being 10 bar above the pressure of the reactor to prevent back pressure. The

second plateau observed after the static extraction represents the dynamic extraction, where continuous CO₂ flow is provided. Dynamic extraction continues for 35 min. After the dynamic extraction, the reactor is depressurized in 14 min.

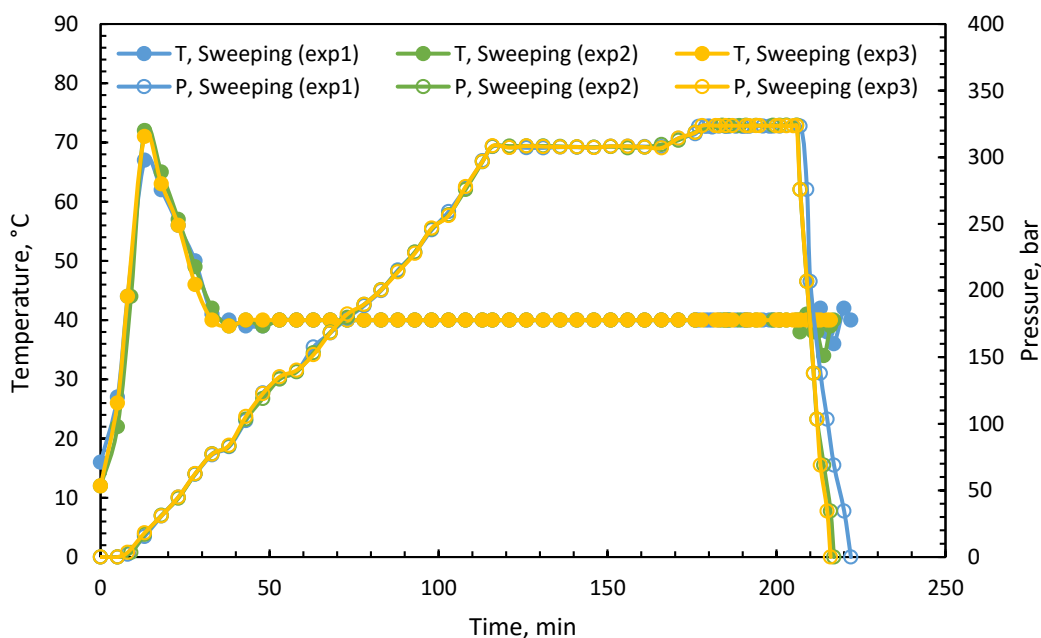


Figure 4.2 Temperature and pressure profiles of the first sweeping experiments of repeatability experiments at 40 °C, 310 bar for 60 min static extraction.

In Figure 4.2, the temperature and pressure profiles of the first sweeping experiments are given. The difference in Figure 4.2 from the previous figure is that reaction does not take place in Figure 4.2. The sweeping experiment starts with heating the empty reactor. The reactor temperature reaches 40 °C in 8 minutes. Then, the reactor is pressurized until the reactor pressure reaches 310 bar. During pressurization, the temperature of the reactor reaches around 70 °C since pressurization causes an increase in temperature. After 30 min, the reactor temperature decreases to 40 °C along with the pressurization. At 116 min, reactor pressure reaches 310 bar and static extraction begins. The first plateau seen in the pressure profile of Figure 4.2 represents the static extraction. A slight pressure increase at the end of the static extraction is due to the pressure of the syringe pump being 16 bar higher than 310

bar to prevent back pressure. The second plateau in the pressure profile is related to the dynamic extraction part of the experiment. After dynamic extraction finishes, the reactor is depressurized in 15 min. Similar behavior for the temperature and pressure profiles of the first sweeping experiment is also observed in the second sweeping experiment, represented in Figure 4.3.

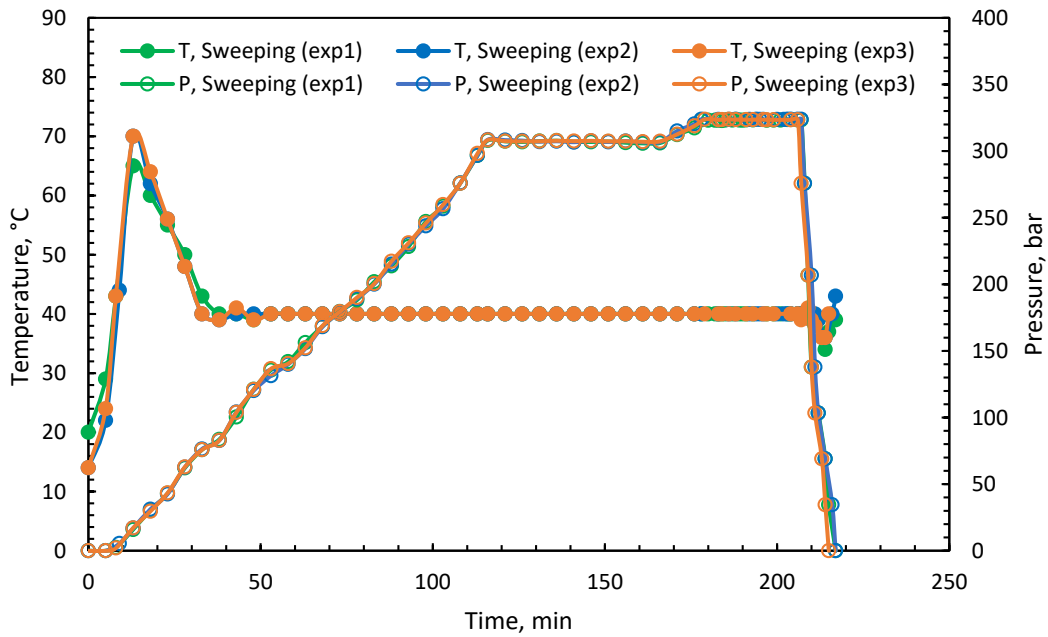


Figure 4.3 Temperature and pressure profiles of the second sweeping experiments of repeatability experiments conducted at 40 °C, 310 bar for 60 min static extraction.

The solid and gas yields obtained for repeatability experiments are detected and presented in Figure 4.4. It is seen that the same gas and solid yields obtained in run 1 were obtained in runs 2 and 3. Gas and solid yields obtained for experimental run 1 are very close to those of runs 2 and 3. On average, 25% gas and 75% solid yields are obtained under these conditions, and average solid yield and gas yield are used to represent the results obtained for extraction conducted at 40 °C, 310 bar for 60 min of static extraction. The error bars are given based on the gas and solid yields obtained from PLA decomposition reactions.

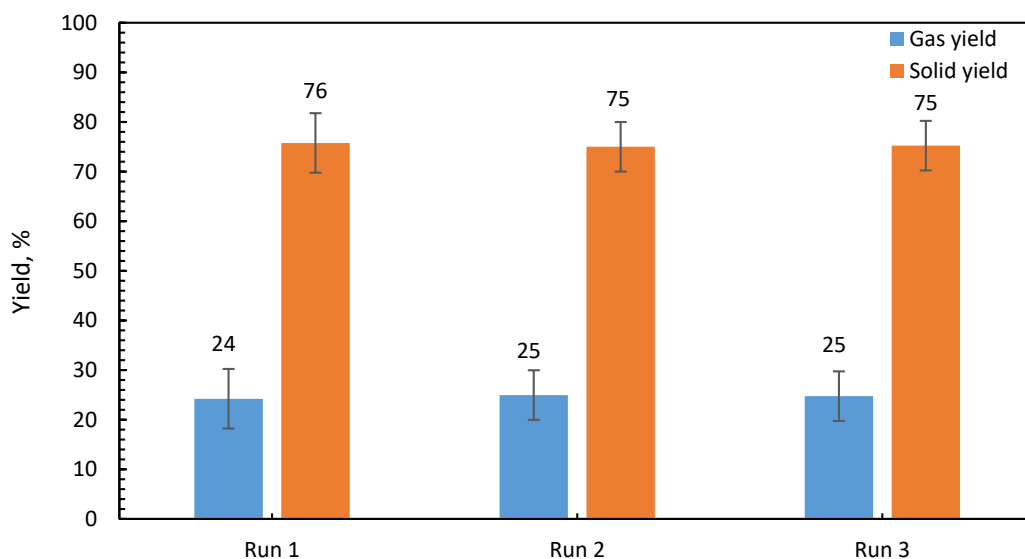


Figure 4.4 Gas and solid yields for the repeatability experiments conducted at 310 bar, 40 °C, and for 60 min of static extraction ($T_{rxn}= 220$ °C, $P_{rxn}=103$ bar, $t_{rxn}= 30$ min.).

The extraction and reactor yields for repeatability experiments are demonstrated in Figure 4.5. The extraction and reactor yields for the repeatability experiments are close to each other with a standard deviation of 3.1 wt.% for both extraction and reactor yields. This value is used in representing the error bars for all extraction and reactor yield results. On average, 63% extraction yield and 37% reactor yield are obtained and these values are used to represent the extraction and reactor yields for the experiment conducted at 40 °C, 310 bar for 60 min of static extraction.

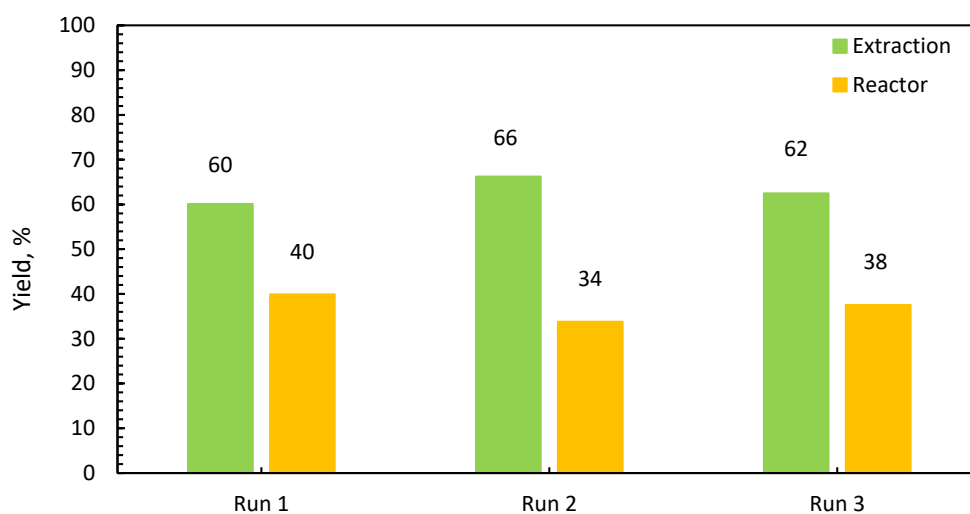


Figure 4.5 Extraction and reactor yields for the repeatability experiments conducted at 310 bar, 40 °C and for 60 min of static extraction ($T_{rxn}= 220\text{ }^{\circ}\text{C}$, $P_{rxn}=103\text{ bar}$, $t_{rxn}= 30\text{ min.}$).

Meso lactide, D, L lactide, lactic acid, and unknown products are detected as the extracted products in the condenser. The retention times of the products are given in Appendix B. The weight % (wt.%) of the product composition obtained in the condenser for the repeatability experiments is shown in Figure 4.6. Similar product compositions for the repeatability experiments are obtained. Five different unknown products which are denoted as UK1, UK2, UK3, UK4, and UK5, are observed for experimental run 1 and run 3. UK 5 is not detected among unknown products for run 2.

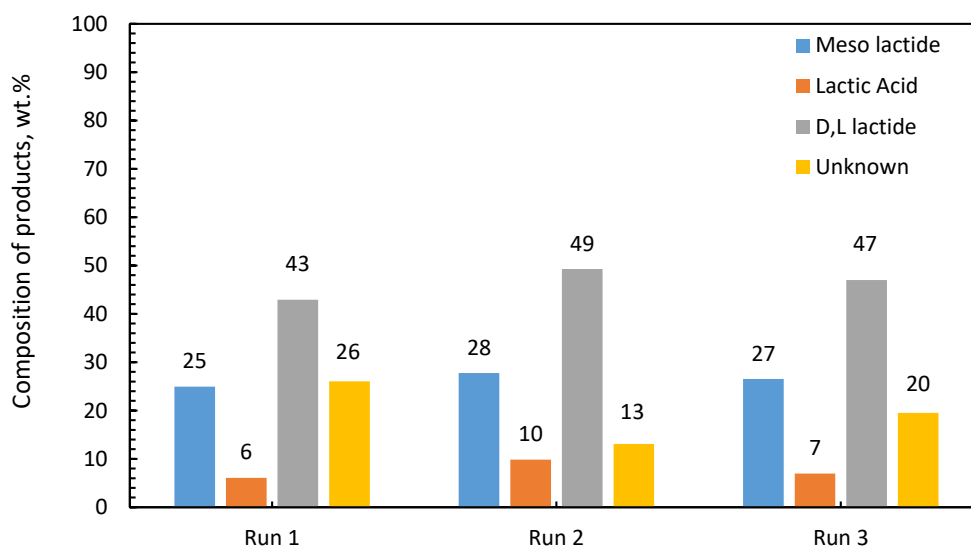


Figure 4.6 Composition of products for the repeatability experiments conducted at 310 bar, 40 °C and for 60 min of static extraction ($T_{rxn}= 220\text{ }^{\circ}\text{C}$, $P_{rxn}=103\text{ bar}$, $t_{rxn}= 30\text{ min.}$).

Averagely, 26% meso lactide, 8% lactic acid, 46% D, L lactide, and 20% unknown products are obtained from the repeatability experiments in the condenser. Standard deviations of 1% for meso lactide, 2% for lactic acid, 3% for D, L lactide, and 6% for unknown products are obtained. Weight% of the unknown products has a pronounced share in condenser composition. This outcome indicates that lactides or lactic acid may be chemically converted into unknown species under these extraction conditions. The average weight % of each product's composition, the extraction, and reactor yields of the repeatability experiments are used to represent the results obtained at 40 °C, 310 bar for 60 min of static extraction in the results provided in this study. The standard deviations of the repeatability experiments are used to represent the error bars of all extraction studies conducted in this study.

4.2 Effect of Extraction Temperature

The influence of the extraction temperature on extraction performance is studied under 40, 60, and 80 °C at 310 bar for 60 min static extraction. The temperature and pressure profiles for the PLA decomposition followed by extraction and the sweeping experiments are represented in Figure 4.7 and Figure 4.8, respectively.

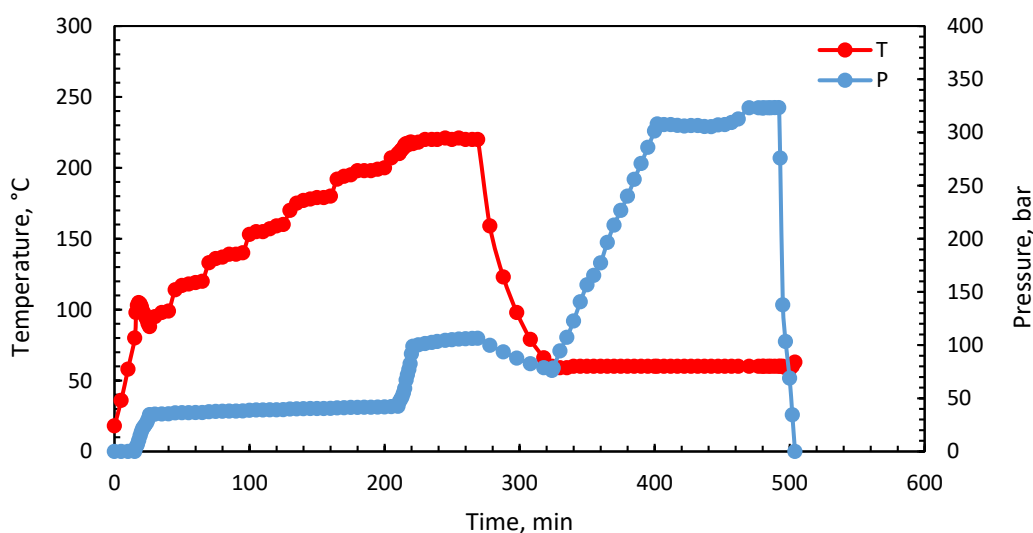


Figure 4.7 Temperature and pressure profile of the experiment with the extraction conducted at 60 °C and 310 bar for 60 min of static extraction.

In Figure 4.7, the reactor is heated and pressurized until reaction conditions are satisfied. The reaction starts at the 240th minute and continues for 30 minutes. After the reaction ends up, the reactor is cooled to 60 °C. Meanwhile, the pressure of the reactor decreases since the reactor temperature decreases. The reactor temperature decreases to 60 °C within 56 min after the reaction finishes. The reactor is pressurized to 310 bar while the reactor temperature is kept constant at 60 °C. Pressurization of the reactor takes 75 min. After pressurization is completed, static extraction begins and continues for 60 min as seen in Figure 4.7. Reactor pressure slightly increases since the pump pressure is adjusted 16 bar higher than the reactor pressure to avoid back pressure. When static extraction ends, the dynamic extraction

part starts and continues for 30 minutes. Then, the reactor is depressurized within 12 minutes.

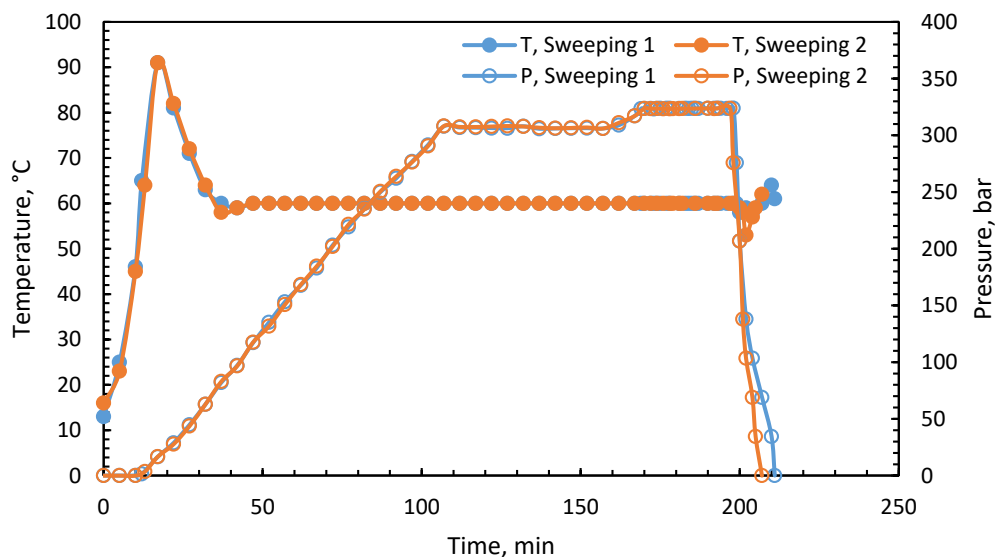


Figure 4.8 Temperature and pressure profiles of sweeping experiments conducted at 310 bar, 60 °C for 60 min of static extraction.

Temperature and pressure profiles of the sweeping experiments for the extraction at 60 °C, and 310 bar for 60 min static extraction are represented in Figure 4.8. Initially, the empty reactor is heated to 60 °C. When the reactor temperature is 60 °C, the reactor is pressurized, and along with the pressurization, the reactor temperature increases to 91 °C. As pressurization continues reactor temperature decreases to 60 °C. Extraction conditions are reached at 107 min. At that time the static extraction begins and continues for 60 min. At the end of the static extraction, dynamic extraction starts with a slight increase of pressure with 16 bar to prevent back pressure. The dynamic extraction part proceeds for 30 min. Then depressurization of the reactor starts and ends in 13 min. The effect of temperature on the gas and solid yields are given in Figure 4.9. The solid yield represents the amount obtained in the condenser together with the amount that remained in the reactor after the extraction is completed. In Figure 4.9, it is observed that as the temperature rises from 40 to 80

°C, gas yield increases. The error bars given in Figure 4.9 represent the deviation of the yields from the reaction yields obtained without the SCCO₂ extraction. When the gas and solid yields of these experiments are compared with those of the depolymerization reaction without SCCO₂ extraction, it is observed that the extracted products which are expected to condense are not adequately trapped in the condenser at higher extraction temperatures, and leave the system as a gas product along with CO₂. This phenomenon can be explained by that the condenser temperature, which is 0 °C or the contact time of products in the condenser is not sufficient enough to condense all the products in the condenser as extraction temperature increases. Therefore, extracted products contribute to the gas yield.

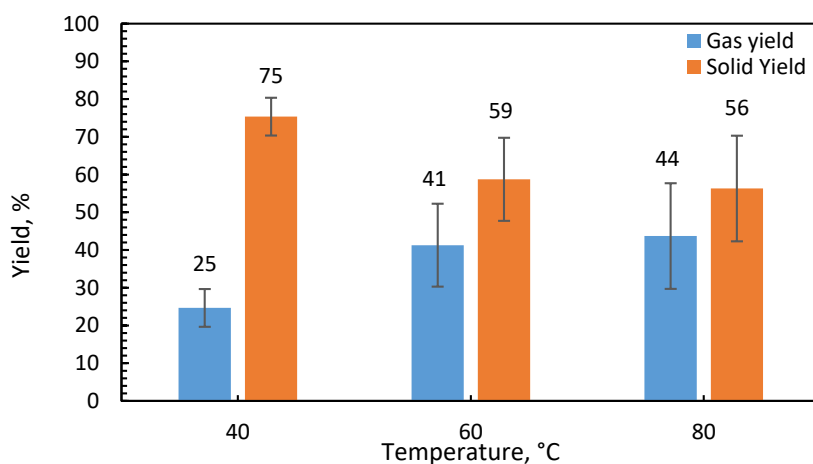


Figure 4.9 The effects of extraction temperature on the gas and solid yields for the SCCO₂ extraction conducted at 310 bar and for 60 min of static extraction ($T_{rxn}=220$ °C, $P_{rxn}=103$ bar, $t_{rxn}=30$ min.).

The extraction yield and reactor yield are calculated based on the amount obtained in the condenser and that remained in the reactor after the extraction process, respectively. The yield results are given in Figure 4.10. The error bars represent the standard deviation of the yields obtained from the repeated extraction experiments carried out at 40 °C, 310 bar, and for 60 min of static extraction.

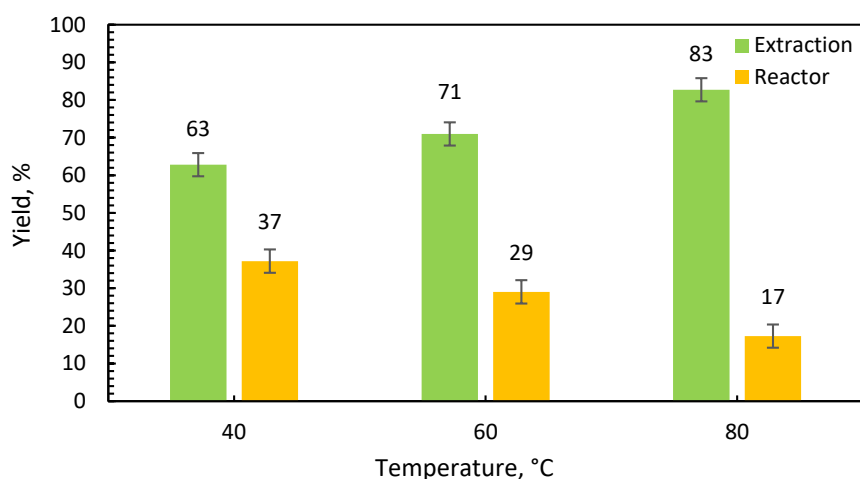


Figure 4.10 The effects of extraction temperature on the extraction and reactor yields for the SCCO₂ extraction conducted at 310 bar and for 60 min of static extraction ($T_{rxn}= 220\text{ }^{\circ}\text{C}$, $P_{rxn}=103\text{ bar}$, $t_{rxn}= 30\text{ min}$).

From Figure 4.10, it is observed that temperature increase provides an enhancement in extraction yields. This improvement may be attributed to the solubility behavior of products in supercritical carbon dioxide. As temperature increases PLA decomposition products such as lactide and lactic acid become more soluble in SCCO₂ (Gregorowicz, 2008), (Gregorowicz, 1999). For this reason, extracted product amount increases, and thus extraction yield enhances. Moreover, temperature rise causes a decrease in the viscosity of the decomposition products in the reactor. As viscosity decreases, mass transfer of the products into the SCCO₂ phase is facilitated. Thus, enhancement in the extraction process leading to an increase in the extracted product amount is observed. As explained earlier some of the extracted products cannot be trapped in the condenser at the higher extraction temperatures, which causes a decrease in the extraction yield. Despite this loss, extraction yields still are observed with an increase in the extraction temperature.

The extracted product distribution from the reactor is given in Figure 4.11. The error bars represent the standard deviation of the yields obtained from the repeated extraction experiments carried out at 40 °C, 310 bar, and for 60 min of static extraction. As the extracted products, meso lactide, D, L lactide, lactic acid, and

unknown products are obtained at all studied extraction temperatures. A slight increase in the composition of D, L lactide, and lactic acid is observed while the composition of meso lactide remains constant as temperature increases. However, a decrease in the percent compositions of the products at 60 °C is observed except for unknown products, which is possibly due to the untrapped products in the condenser, leaving along CO₂ discharge. When the compositions obtained at 80 °C are compared with those obtained at 40 °C, the composition of the CO₂-soluble products, i.e. D, L lactide, and lactic acid are observed to be slightly increased despite the loss due to untrapped extractable products. As explained earlier, this can be attributed to the solubility increase with temperature increase and decrease in the viscosity of the products in the extraction medium with temperature, leading to enhanced mass transfer. Another important observation was related to the types of unknown products. At all extraction temperatures, the formation of various unknown products is observed. At 40 °C, 5 different unknown products, UK1, UK2, UK3, UK4, and UK5 are observed in the extracted products, while UK1, UK2, UK3, UK4, and UK6 are detected at 80 °C. Compared to unknown products obtained in the condenser at 40 and 80 °C, more unknown product species, which are UK1, UK2, UK3, UK4, UK5, UK6, and additionally UK7, are detected. This outcome can explain the higher weight percentage for unknown products at 60 °C. This may show that some of the PLA depolymerization products may be chemically transformed into other species during the extraction process.

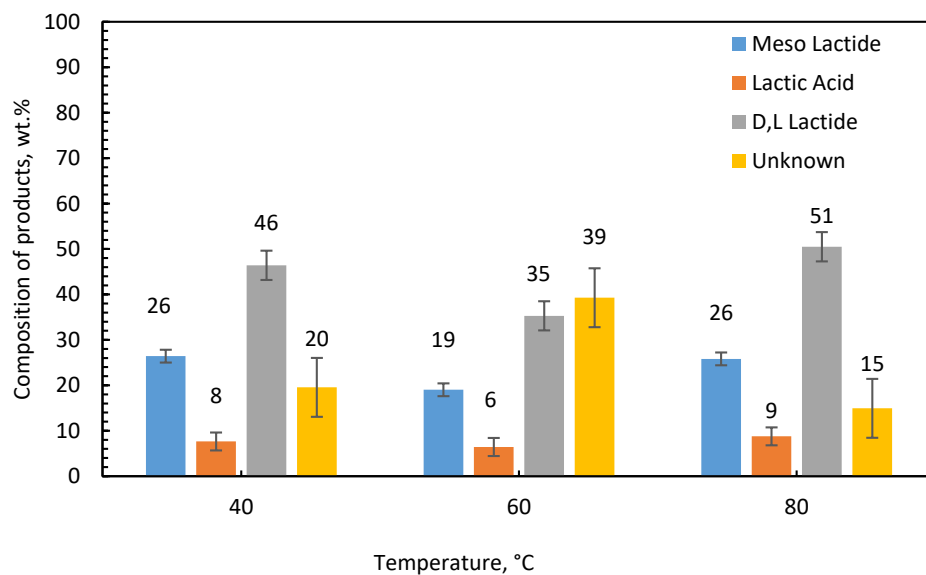


Figure 4.11 Effect of extraction temperature on product distribution of the extracted products at 310 bar for 60 min of static extraction ($T_{rxn}= 220\text{ }^{\circ}\text{C}$, $P_{rxn}=103\text{ bar}$, $t_{rxn}= 30\text{ min.}$).

4.3 Effect of Static Extraction Time

Another studied parameter for the extraction process is the time of the static extraction. The effect of time is investigated at two different temperatures as 40 and 80 °C for 60 and 120 min keeping the extraction pressure at 310 bar. The temperature and pressure profiles for the PLA decomposition followed by extraction and the sweeping experiments conducted at 80 °C for a static extraction time of 120 min are represented in Figure 4.12 and Figure 4.13, respectively.

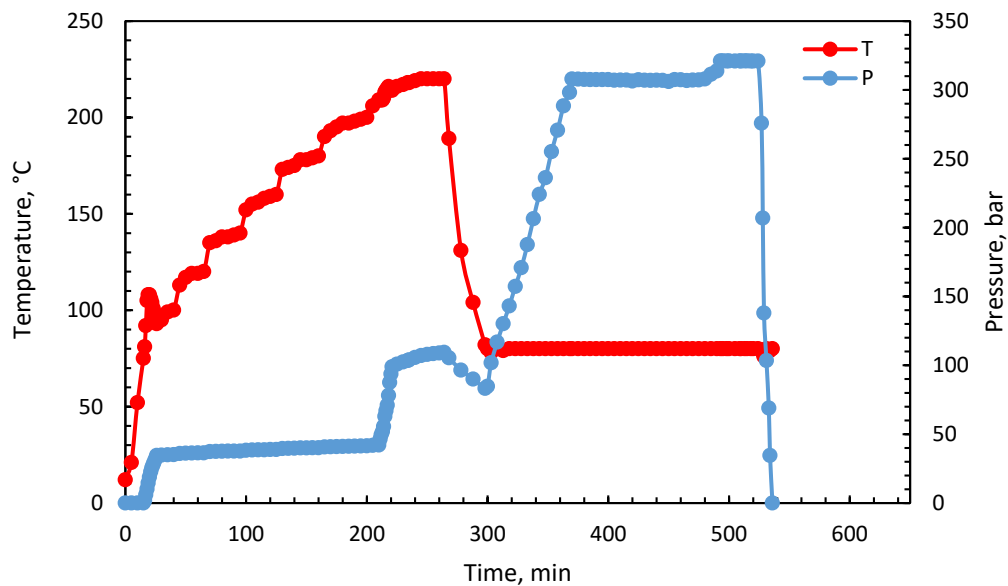


Figure 4.12 Temperature and pressure profile of the experiment with the extraction conducted at 80 °C and 310 bar and for 120 min of static extraction.

As seen in Figure 4.12, PLA pellets are introduced to the reactor, and reaction conditions are satisfied at 235 min. Temperature is kept constant at reaction conditions. Meanwhile, a slight increase in pressure is observed due to the formation of gas products. After 30 min, the reaction ends up and the reactor is cooled to 80 °C in 36 min. Then, the reactor is pressurized to 310 bar within 70 min while the temperature is kept at 80 °C. After pressurization is completed, static extraction starts and continues for 120 min at 80 °C and 310 bar. At the end of the static extraction, pressure moderately increases since the syringe pump pressure is 14 bar higher than the reactor pressure to avoid back pressure. After 120 min of static extraction, dynamic extraction starts and sustains for 34 min. When dynamic extraction ends, the reactor is depressurized within 12 min.

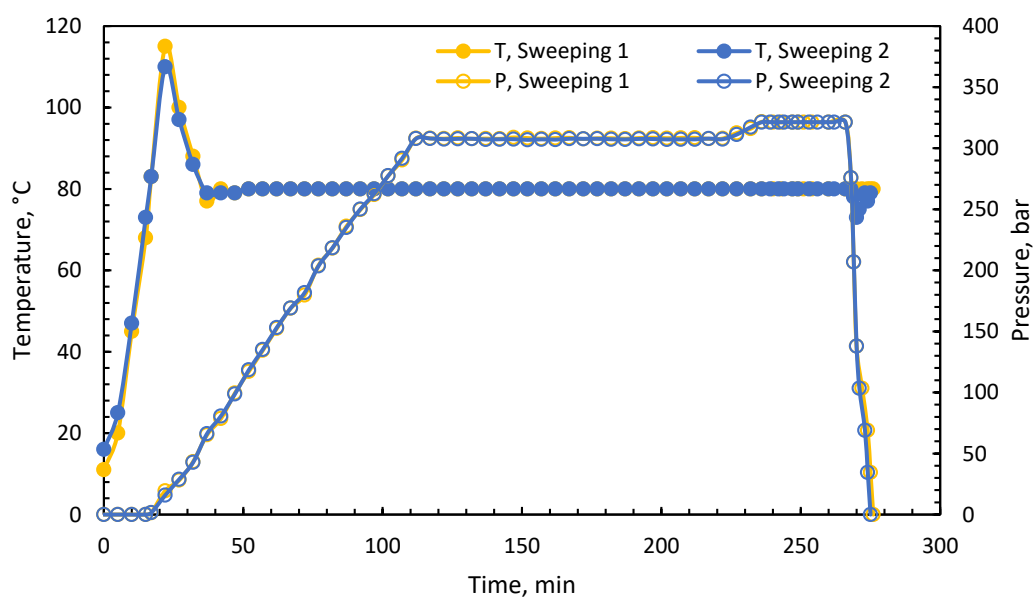


Figure 4.13 Temperature and pressure profiles of sweeping experiments conducted at 310 bar, 80 °C for 120 min of static extraction.

In Figure 4.13, temperature and pressure profiles for sweeping experiments are given. Initially, the empty reactor is heated until the temperature of the reactor is 80 °C. After the reactor temperature reaches 80 °C, the reactor is pressurized until 310 bar. During pressurization, the temperature of the reactor initially increases to 115 °C and then decreases to 80 °C. Pressurization finishes at time 107 min. Then, the static extraction part begins and continues for 120 min as seen from the figure. After 120 min of static extraction, pressure increases slightly before the dynamic extraction due to the 14 bar higher pressure of the syringe pump to prevent back pressure. Then, dynamic extraction starts and continues for 34 min. After dynamic extraction ends, the pressure of the reactor starts to decrease. Depressurization is completed within 10 min.

Solid and gas yields obtained with SCCO₂ extraction experiments conducted at 40 and 80 °C are represented in Figure 4.14 and Figure 4.15, respectively. The error

bars given in the figures represent the deviation of the yields from the reaction yields obtained without the SCCO₂ extraction.

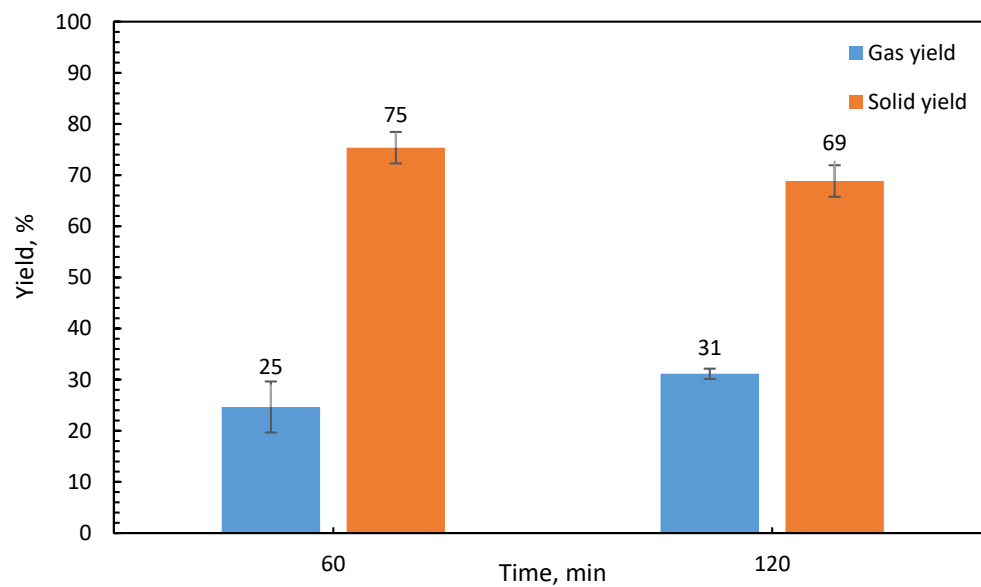


Figure 4.14 The effects of static extraction time on the gas and solid yields for the SCCO₂ extraction conducted at 40 °C and 310 bar ($T_{rxn}= 220$ °C, $P_{rxn}=103$ bar, $t_{rxn}= 30$ min.).

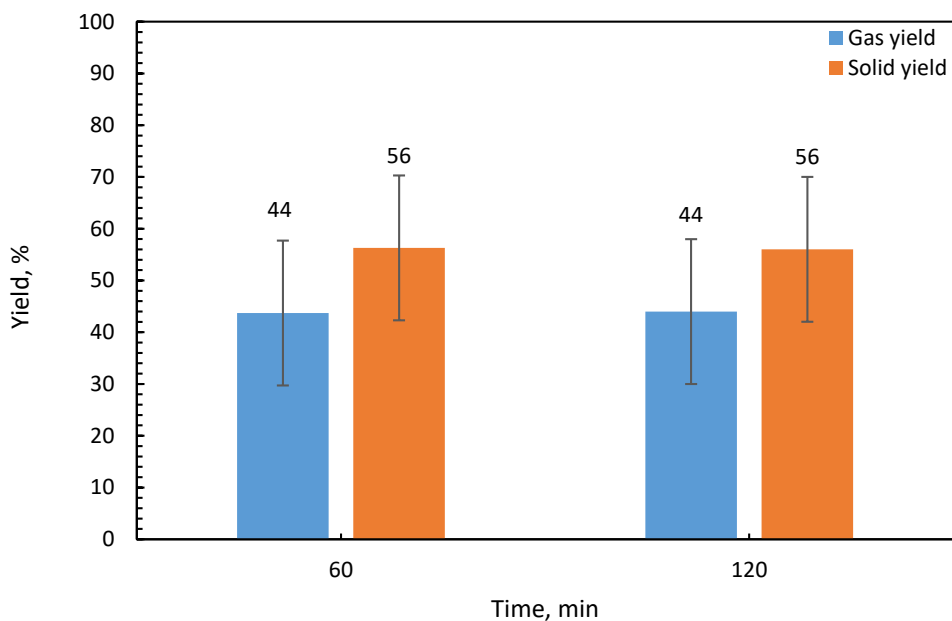


Figure 4.15 The effects of static extraction time on the gas and solid yields for the SCCO₂ extraction conducted at 80 °C and 310 bar ($T_{rxn}= 220\text{ °C}$, $P_{rxn}=103\text{ bar}$, $t_{rxn}= 30\text{ min.}$).

According to the results shown in Figure 4.14, as the extraction time increases gas yield increases and solid yield decreases slightly. At 40 °C, in a longer extraction time, more products are expected to transfer into the SCCO₂. Therefore, an increase in the amount of untrapped products is expected. For this reason, an increase in gas yield with longer extraction time occurs. As for Figure 4.15, the gas yield and solid yield remained unchanged at 80 °C. The effect of static extraction time is not reflected in this figure since it is more difficult to condense the extracted products at 80 °C, as it requires longer contact time or lower condenser temperature. The effect of time is suppressed by the significant amount lost with the CO₂ release.

The effect of static extraction time on the extraction and reactor yields at 40 and 80 °C are given in Figure 4.16 and Figure 4.17, respectively. The error bars represent the standard deviation of the yields obtained from the repeated extraction experiments carried out at 40 °C, 310 bar, and for 60 min of static extraction.

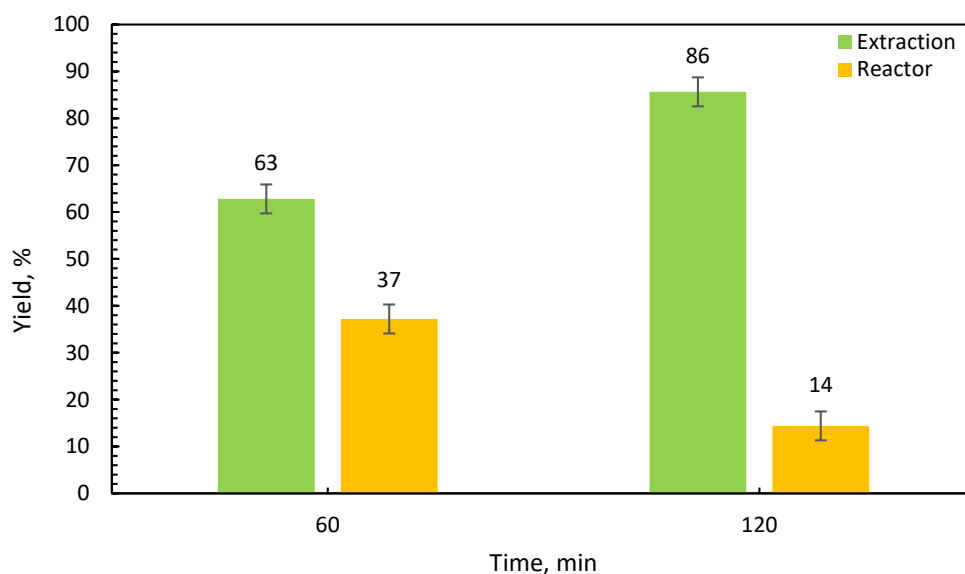


Figure 4.16 The effects of static extraction time on the extraction and reactor yields for the SCCO₂ extraction conducted at 40 °C and 310 bar ($T_{rxn} = 220$ °C, $P_{rxn} = 103$ bar, $t_{rxn} = 30$ min.).

From Figure 4.16, it is seen that as extraction time is increased from 60 to 120 min, the amount of the extracted products in the condenser increases, and thus extraction yield increases. Longer extraction time provides more sufficient time for the products to dissolve into the SCCO₂ phase. Consequently, more product amount is observed in the condenser. This trend is slightly seen when the extraction is conducted at 80 °C (Figure 4.17) due to the suppressing effect of the untrapped products lost with the CO₂ release. The condensation of the extracted products at 80 °C is more difficult compared to 40 °C. In other words, some of the extracted products leave the system without condensation.

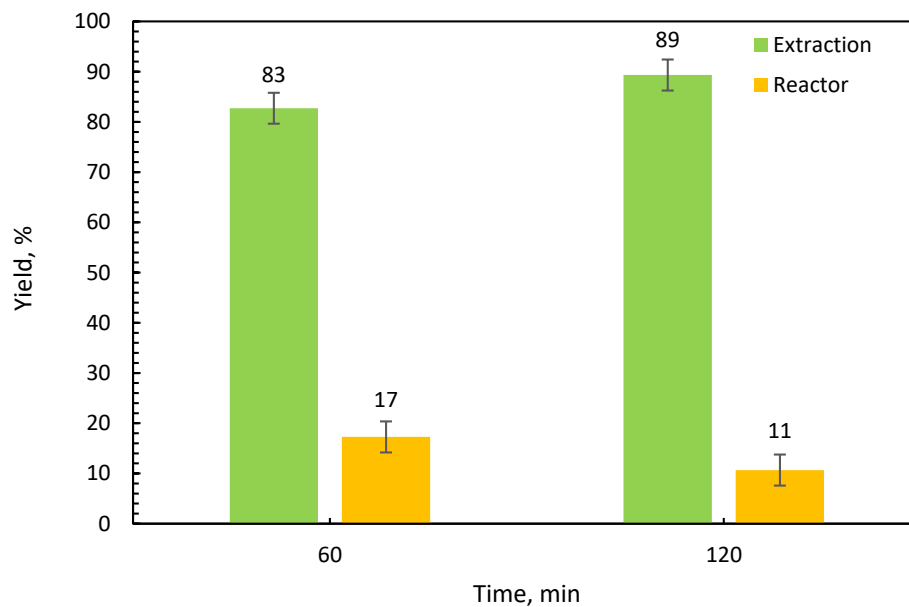


Figure 4.17 The effects of static extraction time on the extraction and reactor yields for the SCCO₂ extraction conducted at 80 °C and 310 bar ($T_{rxn} = 220$ °C, $P_{rxn} = 103$ bar, $t_{rxn} = 30$ min.).

The effect of static extraction time on the extracted product distribution from the reactor is given in Figure 4.18 and Figure 4.19 for two different extraction temperatures of 40 and 80 °C, respectively. The error bars represent the standard deviation of the yields obtained from the repeated extraction experiments carried out at 40 °C, 310 bar, and for 60 min of static extraction.

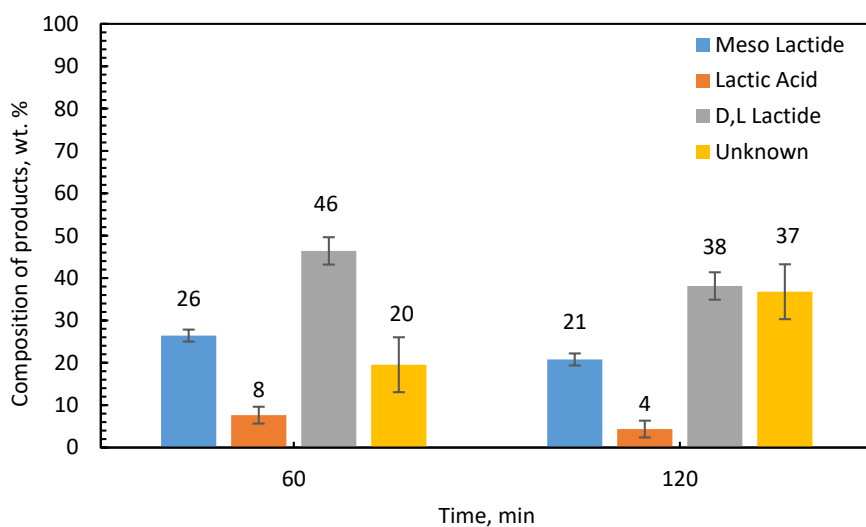


Figure 4.18 Effect of static extraction time on product distribution of the extracted products at 40 °C and 310 bar ($T_{rxn}= 220$ °C, $P_{rxn}=103$ bar, $t_{rxn}= 30$ min.).

Products detected in the condenser are composed of meso lactide, D, L lactide, lactic acid, and unknown products at 40 °C as seen in Figure 4.18. When the extraction time is increased from 60 to 120 min, the composition of each extractable product is expected to increase. However, this expectation is not satisfied with the composition results in Figure 4.18. This may show that some of the products obtained from PLA depolymerization may be chemically transformed into other chemicals during the longer extraction process. UK1, UK2, UK3, UK4, and UK5 constitute the unknown product composition obtained in the experiment with static extraction of 60 min. On the other hand, only UK1, UK2, and UK3 are detected in the experiment with 120 min of static extraction.

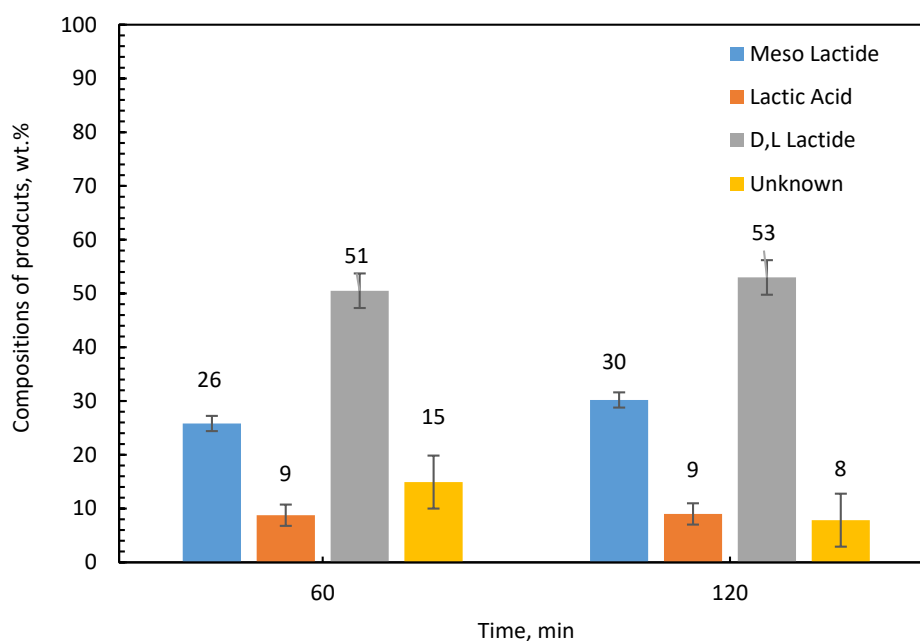


Figure 4.19 Effect of static extraction time on product distribution of the extracted products at 80 °C and 310 bar ($T_{rxn}= 220\text{ °C}$, $P_{rxn}=103\text{ bar}$, $t_{rxn}= 30\text{ min.}$)

Condenser composition is composed of meso lactide, lactic acid, D, L lactide, and unknown products. Similarly, the effect of time is not observed as seen in Figure 4.19. Similar behavior is observed in the SCCO₂ extraction experiments conducted at 80 °C due to the problems in trapping the extractable products in the condenser and possible chemical reactions of the extractable products leading to the formation of other chemicals during the longer extraction process. The unknown product obtained in the experiment with static extraction of 60 min is composed of UK1, UK2, UK3, UK4, and UK6 while UK1, UK2, UK3, and UK4 are the unknown products observed in the experiment with the 120 min of static extraction.

4.4 Effect of Extraction Pressure

The effect of extraction pressure on the extraction performance is studied at 40 °C for 60 min of static extraction time at two different pressures, which are 241 and 310 bar. The temperature and pressure profiles for the PLA decomposition followed by extraction and the sweeping experiments conducted at 241 bar are represented in Figure 4.20 and Figure 4.21, respectively for 241 bar.

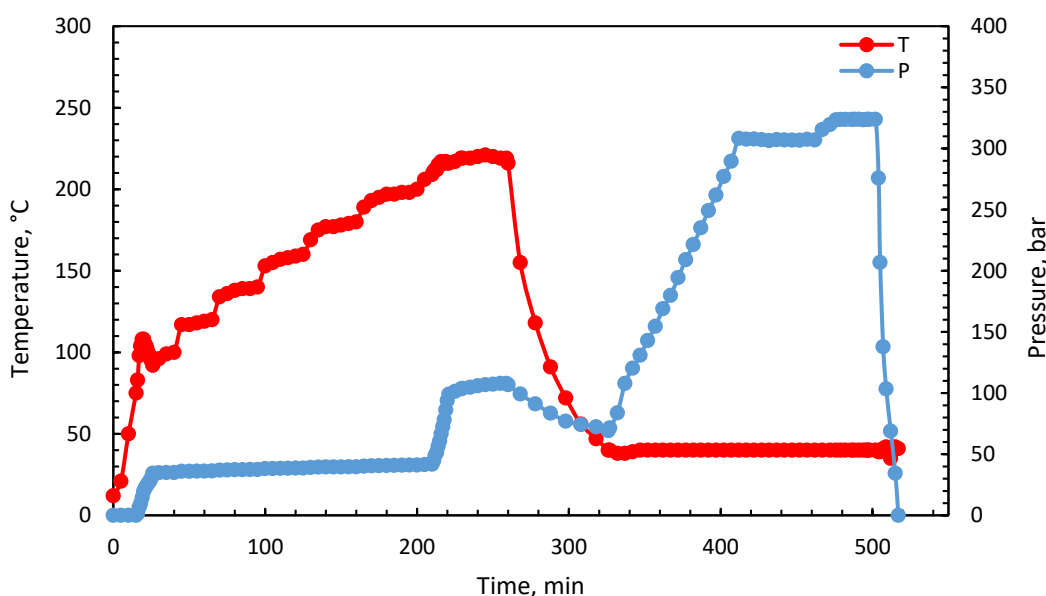


Figure 4.20 Temperature and pressure profile of the extraction experiment conducted at 40 °C and 241 bar and for 60 min of static extraction.

As seen in Figure 4.20, the reactor which contains PLA pellets is heated and pressurized to reaction conditions. Reaction conditions are attained at time 237 min. At this time, the reaction starts and ends at time 267 min. During the reaction, the temperature is constant at 220 °C and pressure slightly increases due to gas product formation as the reaction proceeds. After the reaction ends, the reactor is cooled to 40 °C within 67 min. Then, the reactor is pressurized up to 241 bar at 40 °C. After reactor pressure reaches 241 bar, static extraction begins (seen in the figure as a plateau). Static extraction takes 60 min. Again, a slight increase in pressure is observed since the syringe pump pressure is 14 bar above the reactor pressure to

avoid back pressure. After static extraction ends, dynamic extraction starts and continues for 34 min. Then, depressurization of the reactor occurs and finishes within 10 min.

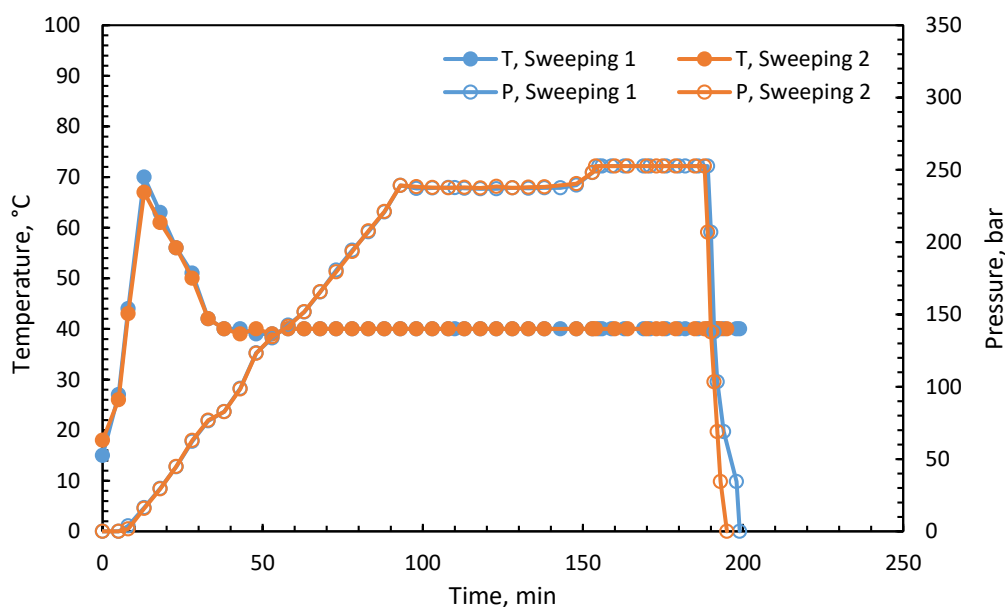


Figure 4.21 Temperature and pressure profile of sweeping experiments conducted at 40 °C at 241 bar and for 60 min of static extraction.

Figure 4.21 represents the temperature and pressure profiles for sweeping experiments at 241 bar. Firstly, the empty reactor is heated until the reactor temperature reaches 40 °C. Next, the reactor is pressurized to 241 bar. During pressurization, the temperature of the reactor initially increases to 73 °C and then decreases to 40 °C. Pressurization finishes at time 93 min. After that, static extraction begins and continues for 60 min as seen from the figure (first plateau of the pressure plot). After 60 min of static extraction, pressure increases slightly before dynamic extraction due to the 14 bar higher pressure of the syringe pump to avoid back pressure. Next, dynamic extraction starts and continues for 34 min. After dynamic extraction ends, the pressure of the reactor starts to decrease. Depressurization is completed within 10 min.

The solid and gas yields obtained with SCCO₂ extraction experiments conducted at 40 °C and two different pressures for 60 min of static extraction are represented in Figure 4.22. The error bars given in the figures represent the deviation of the yields from the reaction yields obtained without the SCCO₂ extraction. The gas and solid yields are very close for both pressure conditions. Pressure increase seems not to be effective in terms of gas and solid yields.

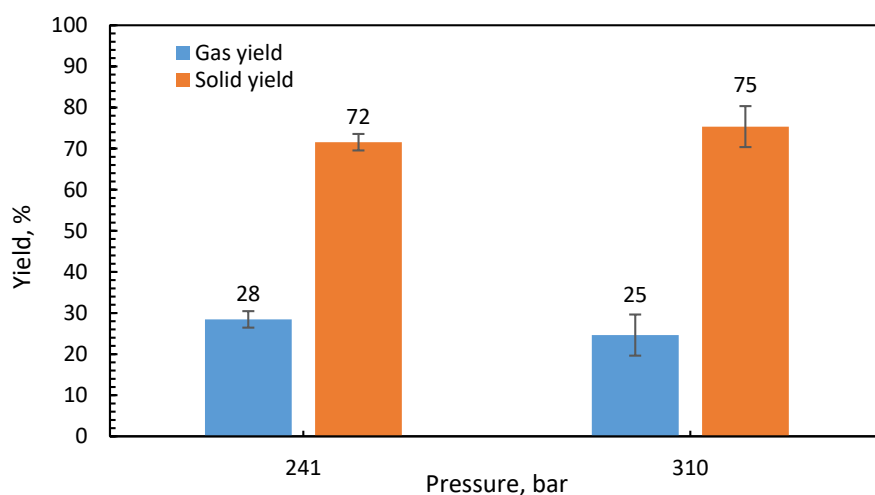


Figure 4.22 The effects of static extraction time on the gas and solid yields for the SCCO₂ extraction conducted at 40 °C for 60 min static extraction ($T_{rxn}= 220$ °C, $P_{rxn}=103$ bar, $t_{rxn}= 30$ min.).

The effect of extraction pressure on the extraction yield is illustrated in Figure 4.23. The error bars represent the standard deviation of the yields obtained from the repeated extraction experiments carried out at 40 °C, 310 bar, and for 60 min of static extraction.

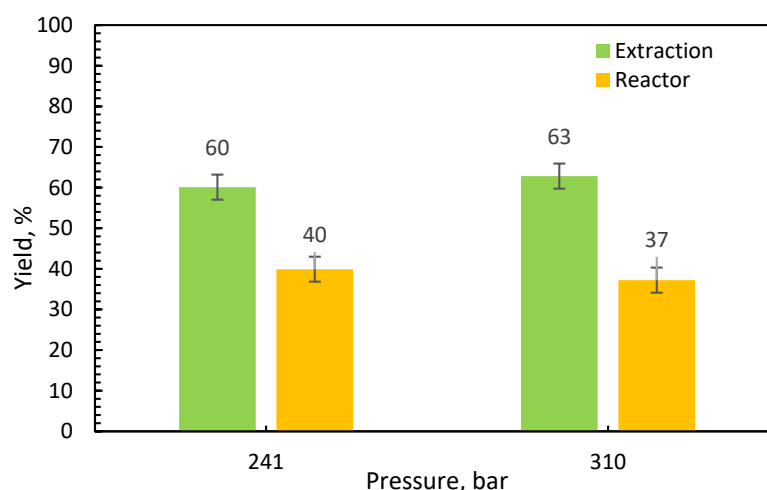


Figure 4.23 The effects of static extraction time on the extraction and reactor yields for the SCCO₂ extraction conducted at 40 °C for 60 min static extraction ($T_{rxn}= 220$ °C, $P_{rxn}=103$ bar, $t_{rxn}= 30$ min.).

The yields obtained at extraction pressures of 241 and 310 bar reveal that no pronounced effect is observed with an increase in pressure. In the selected pressures, the products are already soluble in CO₂ under these pressures. Only a slight increase in extraction yield with pressure may be related to the enhancement in the mass transfer of the products into the SCCO₂ phase due to the higher dissolution of CO₂ in the reaction mixture leading to a possible slight decrease in the viscosity of the reaction mixture.

The effect of extraction pressure on the extracted product distribution from the reactor is given in Figure 4.24. The error bars represent the standard deviation of the yields obtained from the repeated extraction experiments carried out at 40 °C, 310 bar, and for 60 min of static extraction.

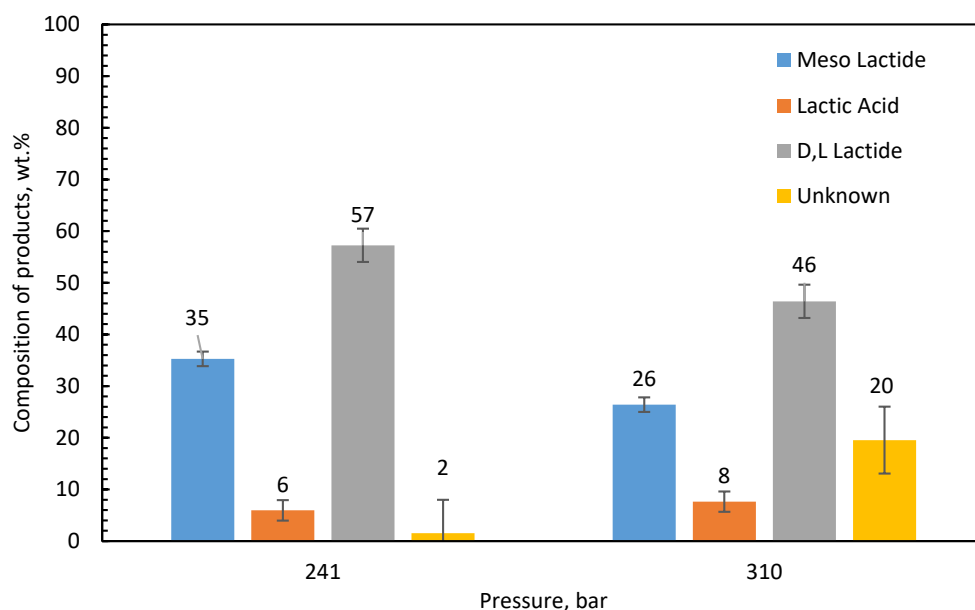


Figure 4.24 Effect of static extraction pressure on product distribution of the extracted products at 40 °C for 60 min of static extraction ($T_{rxn}= 220$ °C, $P_{rxn}=103$ bar, $t_{rxn}= 30$ min.)

Meso lactide, D, L lactide, lactic acid, and unknown products are observed in the condenser. When the extraction pressure is increased from 241 bar to 310 bar, the composition of each extractable product is observed to decrease along with the further formation of unknown products, which may show that some of the products obtained from PLA depolymerization may be chemically transformed into other chemicals during the extraction process. UK1, UK2, and UK3 are the unknown products observed when the extraction pressure is 241 bar. On the other hand, UK1, UK2, UK3, UK4, and UK5 are detected in the unknown products at 310 bar.

CHAPTER 5

CONCLUSIONS

In this thesis study, environmentally benign extraction of PLA decomposition products from the reaction environment is investigated. PLA decomposition experiments are conducted in supercritical carbon dioxide. With the PLA decomposition reactions, PLA is converted into gas and highly viscous fluid which is referred to as solid. 70% solid and 30% gas yields are obtained with the decomposition reactions where no SCCO₂ extraction was applied. Then, the SCCO₂ extraction of the products is investigated based on three critical variables, temperature, time, and pressure.

The obtained extraction yields at different temperatures indicate that enhancement in extraction yield is observed with extraction temperature due to an increase in the solubility of the products in SCCO₂ and the decrease in the viscosity of the reaction medium facilitating the mass transfer of the extractable products into the SCCO₂ phase.

The extraction yield increases with increasing static extraction time. As extraction time increases, more products can dissolve in SCCO₂. Thus, the amount of extracted product and extraction yield increase.

An increase in extraction pressure slightly increases the extraction yield. Although the solubility of the products increases when pressure is increased, only a slight enhancement is observed, indicating that the pressure is not enough to speed up the mass transfer of the products. It should be supported by extraction time and temperature.

As the extracted products, meso lactide, D, L lactide, lactic acid, and some unknown products are detected. The formation of some unknown products in the extracted

products indicates that the SCCO₂ extraction may lead to some chemical transformation of products to other species.

Among the SCCO₂ extraction parameters, extraction temperature has the greatest influence on the extraction of the products from the reaction mixture. Extraction experiments demonstrate extraction temperature is the most influencing parameter for the extraction process compared to time, and pressure. Extraction at 80 °C, 310 bar for 2 hours results in 89% extraction yield. The product obtained in a condenser under these conditions is composed of 30% meso lactide, 9% lactic acid, 53% D, L lactide, and 8% unknown products.

CHAPTER 6

RECOMMENDATIONS

This thesis study aims to develop an environmentally friendly separation process of PLA degradation products without using an organic solvent or water. For the extraction of the PLA degradation products, a SCCO₂ extraction process is developed. For this purpose, extraction parameters such as temperature, pressure, and time are employed to investigate the effects of the parameters on the extraction performance. However, at some process conditions, especially at higher extraction temperatures, some of the extracted products are observed to be untrapped in the condenser and lost along with the CO₂ release. Therefore, some suggestions are proposed to improve the extraction system.

The condenser system can be modified by two means, which are decreasing the cooling water temperature and increasing the contact time between the CO₂ release including extracted products and cooling water. The contact time can be increased either by modifying the condenser geometry or by decreasing the CO₂ release flow rate during the dynamic extraction.

Another suggestion is related to unknown products. For further analysis of unknown products, GC-MS can be used to detect unknown species.

REFERENCES

- Auras, R., Harte, B., & Selke, S. (2004). An overview of polylactides as packaging materials. *Macromolecular Bioscience*, 4(9), 835–864. <https://doi.org/10.1002/mabi.200400043>
- Badia, J. D., & Ribes-Greus, A. (2016). Mechanical recycling of polylactide, upgrading trends and combination of valorization techniques. *European Polymer Journal*, 84, 22–39. <https://doi.org/10.1016/j.eurpolymj.2016.09.005>
- Baiker, A. (1999). Supercritical Fluids in Heterogeneous Catalysis. *Chemical Reviews*, 99(2–3), 453–473. <https://doi.org/10.1021/cr970090z>
- Boonluksiri, Y., Prapagdee, B., & Sombatsompop, N. (2021). Promotion of polylactic acid biodegradation by a combined addition of PLA-degrading bacterium and nitrogen source under submerged and soil burial conditions. *Polymer Degradation and Stability*, 188. <https://doi.org/10.1016/j.polymdegradstab.2021.109562>
- Calvo-Flores, F. G., Monteagudo-Arrebola, M. J., Dobado, J. A., & Isac-García, J. (2018). Green and Bio-Based Solvents. *Topics in Current Chemistry*, 376(3), 1–40. <https://doi.org/10.1007/s41061-018-0191-6>
- Castro-Aguirre, E., Iñiguez-Franco, F., Samsudin, H., Fang, X., & Auras, R. (2016). Poly(lactic acid)—Mass production, processing, industrial applications, and end of life. *Advanced Drug Delivery Reviews*, 107, 333–366. <https://doi.org/10.1016/j.addr.2016.03.010>
- Chemical Sciences and Society Summit. (2020). *Science to Enable Sustainable Plastics - A white paper from the 8th Chemical Sciences and Society Summit (CS3)* (Issue 2). rsc.li/sustainable-plastics-report
- Clercq, R. De, Dusselier, M., Poleunis, C., Debecker, D. P., Giebeler, L., Makshina, E., & Sels, B. F. (2018). Titania-Silica Catalysts for Lactide Production from Renewable Alkyl Lactates: Structure – Activity Relations. *ACS Catalysis*, 8(9),

8130–8139. <https://doi.org/10.1021/acscatal.8b02216>

- Cristina, A. M., Sara, F., Fausto, G., Vincenzo, P., Rocchina, S., & Claudio, V. (2018). Degradation of Post-consumer PLA: Hydrolysis of Polymeric Matrix and Oligomers Stabilization in Aqueous Phase. *Journal of Polymers and the Environment*, 26(12), 4396–4404. <https://doi.org/10.1007/s10924-018-1312-6>
- Cvjetko Bubalo, M., Vidović, S., Radojčić Redovniković, I., & Jokić, S. (2015). Green solvents for green technologies. *Journal of Chemical Technology and Biotechnology*, 90(9), 1631–1639. <https://doi.org/10.1002/jctb.4668>
- Datta, R., & Henry, M. (2006). Lactic acid : recent advances in products , processes and technologies – a review. *Journal of Chemical Technology and Biotechnology*, 81(7), 1119–1129. <https://doi.org/10.1002/jctb>
- Elmanovich, I. V., Stakhanov, A. I., Kravchenko, E. I., Stakhanova, S. V., Pavlov, A. A., Ilyin, M. M., Kharitonova, E. P., Gallyamov, M. O., & Khokhlov, A. R. (2022). Chemical recycling of polyethylene in oxygen-enriched supercritical CO₂. *Journal of Supercritical Fluids*, 181(December 2021), 105503. <https://doi.org/10.1016/j.supflu.2021.105503>
- Elmanovich, I. V., Stakhanov, A. I., Zefirov, V. V., Pavlov, A. A., Lokshin, B. V., & Gallyamov, M. O. (2020). Thermal oxidation of polypropylene catalyzed by manganese oxide aerogel in oxygen-enriched supercritical carbon dioxide. *Journal of Supercritical Fluids*, 158, 104744. <https://doi.org/10.1016/j.supflu.2019.104744>
- Elsawy, M. A., Kim, K. H., Park, J. W., & Deep, A. (2017). Hydrolytic degradation of polylactic acid (PLA) and its composites. *Renewable and Sustainable Energy Reviews*, 79(May), 1346–1352. <https://doi.org/10.1016/j.rser.2017.05.143>
- Essien, S. O., Young, B., & Baroutian, S. (2020). Recent advances in subcritical water and supercritical carbon dioxide extraction of bioactive compounds from plant materials. *Trends in Food Science and Technology*, 97(January), 156–169. <https://doi.org/10.1016/j.tifs.2020.01.014>

- European Bioplastics. (2020). *Bioplastics market development update 2020*.
<https://www.european-bioplastics.org/news/publications/#MarketData>
- Fan, Y., Nishida, H., Mori, T., Shirai, Y., & Endo, T. (2004). Thermal degradation of poly(L-lactide): Effect of alkali earth metal oxides for selective L,L-lactide formation. *Polymer*, *45*(4), 1197–1205.
<https://doi.org/10.1016/j.polymer.2003.12.058>
- Farah, S., Anderson, D. G., & Langer, R. (2016). Physical and mechanical properties of PLA, and their functions in widespread applications — A comprehensive review. *Advanced Drug Delivery Reviews*, *107*, 367–392.
<https://doi.org/10.1016/j.addr.2016.06.012>
- Gironi, F., & Piemonte, V. (2011). Bioplastics and petroleum-based plastics: Strengths and weaknesses. *Energy Sources, Part A: Recovery, Utilization and Environmental Effects*, *33*(21), 1949–1959.
<https://doi.org/10.1080/15567030903436830>
- Gregorowicz, J. (1999). Solubilities of lactic acid and 2-hydroxyhexanoic acid in supercritical CO₂. *Fluid Phase Equilibria*, *166*(1), 39–46.
[https://doi.org/10.1016/S0378-3812\(99\)00283-6](https://doi.org/10.1016/S0378-3812(99)00283-6)
- Gregorowicz, J. (2008). Phase behaviour of l-lactide in supercritical carbon dioxide at high pressures. *Journal of Supercritical Fluids*, *46*(2), 105–111.
<https://doi.org/10.1016/j.supflu.2008.04.004>
- Gupta, A. P., & Kumar, V. (2007). New emerging trends in synthetic biodegradable polymers - Polylactide: A critique. *European Polymer Journal*, *43*(10), 4053–4074. <https://doi.org/10.1016/j.eurpolymj.2007.06.045>
- Hajjighasemi, M., Nocek, B. P., Tchigvintsev, A., Brown, G., Flick, R., Xu, X., Cui, H., Hai, T., Joachimiak, A., Golyshin, P. N., Savchenko, A., Edwards, E. A., & Yakunin, A. F. (2016). Biochemical and Structural Insights into Enzymatic Depolymerization of Polylactic Acid and Other Polyesters by Microbial Carboxylesterases. *Biomacromolecules*, *17*(6), 2027–2039.
<https://doi.org/10.1021/acs.biomac.6b00223>

- Henton, D. E., Gruber, P., Lunt, J., & Randall, J. (2005). Polylactic acid technology. *Natural Fibers, Biopolymers, and Biocomposites*, 48674(23), 527–577. [https://doi.org/10.1002/1521-4095\(200012\)12:23<1841::aid-adma1841>3.3.co;2-5](https://doi.org/10.1002/1521-4095(200012)12:23<1841::aid-adma1841>3.3.co;2-5)
- Herrero, M., Mendiola, J. A., Cifuentes, A., & Ibáñez, E. (2010). Supercritical fluid extraction: Recent advances and applications. *Journal of Chromatography A*, 1217(16), 2495–2511. <https://doi.org/10.1016/j.chroma.2009.12.019>
- Hirao, K., Nakatsuchi, Y., & Ohara, H. (2010). Alcoholysis of Poly(l-lactic acid) under microwave irradiation. *Polymer Degradation and Stability*, 95(6), 925–928. <https://doi.org/10.1016/j.polymdegradstab.2010.03.027>
- Jarerat, A., & Tokiwa, Y. (2001). Degradation of Poly(L-lactide) by a Fungus. *Macromolecular Bioscience*, 1(4), 136–140. [https://doi.org/10.1002/1616-5195\(20010601\)1:4<136::AID-MABI136>3.0.CO;2-3](https://doi.org/10.1002/1616-5195(20010601)1:4<136::AID-MABI136>3.0.CO;2-3)
- Jarerat, A., & Tokiwa, Y. (2003). Poly (L-lactide) degradation by *Saccharothrix waywayandensis*. *Biotechnology Letters*, 25, 401–404. <https://doi.org/10.1023/A:1022450431193>
- Jarerat, A., Tokiwa, Y., & Tanaka, H. (2003). Poly (L-lactide) degradation by *Kibdelosporangium aridum*. *Biotechnology Letters*, 25, 2035–2038. <https://doi.org/10.1023/B:BILE.0000004398.38799.29>
- Jarerat, A., Tokiwa, Y., & Tanaka, H. (2004). Microbial Poly (L-lactide) -Degrading Enzyme Induced by Amino Acids , Peptides , and Poly (L-amino Acids). *Polymers and the Environment*, 12, 139–146. <https://doi.org/10.1023/B:JOOE.0000038545.69235.f2>
- Jem, K. J., & Tan, B. (2020). The development and challenges of poly (lactic acid) and poly (glycolic acid). *Advanced Industrial and Engineering Polymer Research*, 3(2), 60–70. <https://doi.org/10.1016/j.aiepr.2020.01.002>
- Kijchavengkul, T., & Auras, R. (2008). Compostability of Polymers. *Polymer International*, 57(6), 793–804. <https://doi.org/10.1002/pi.2420>

- Knez, Markočič, E., Leitgeb, M., Primožič, M., Knez Hrnčič, M., & Škerget, M. (2014). Industrial applications of supercritical fluids: A review. *Energy*, 77, 235–243. <https://doi.org/10.1016/j.energy.2014.07.044>
- Lamberti, F. M., Román-Ramírez, L. A., Mckeown, P., Jones, M. D., & Wood, J. (2020). Kinetics of alkyl lactate formation from the alcoholysis of poly(lactic acid). *Processes*, 8(6). <https://doi.org/10.3390/PR8060738>
- Lamberti, F. M., Román-Ramírez, L. A., & Wood, J. (2020). Recycling of Bioplastics: Routes and Benefits. *Journal of Polymers and the Environment*, 28(10), 2551–2571. <https://doi.org/10.1007/s10924-020-01795-8>
- Leejarkpai, T., Suwanmanee, U., Rudeekit, Y., & Mungcharoen, T. (2011). Biodegradable kinetics of plastics under controlled composting conditions. *Waste Management*, 31(6), 1153–1161. <https://doi.org/10.1016/j.wasman.2010.12.011>
- Leitner, W. (2002). Supercritical carbon dioxide as a green reaction medium for catalysis. *Accounts of Chemical Research*, 35(9), 746–756. <https://doi.org/10.1021/ar010070q>
- Liu, F., Guo, J., Zhao, P., Gu, Y., Gao, J., & Liu, M. (2019). Facile synthesis of DBU-based protic ionic liquid for efficient alcoholysis of waste poly (lactic acid) to lactate esters. *Polymer Degradation and Stability*, 167, 124–129. <https://doi.org/10.1016/j.polymdegradstab.2019.06.028>
- Liu, H., Song, X., Liu, F., Liu, S., & Yu, S. (2015). Ferric chloride as an efficient and reusable catalyst for methanolysis of poly(lactic acid) waste. *Journal of Polymer Research*, 22(135). <https://doi.org/10.1007/s10965-015-0783-6>
- Liu, H., Zhao, R., Song, X., Liu, F., Yu, S., Liu, S., & Ge, X. (2017). Lewis Acidic Ionic Liquid [Bmim]FeCl₄ as a High Efficient Catalyst for Methanolysis of Poly (lactic acid). *Catalysis Letters*, 147(9), 2298–2305. <https://doi.org/10.1007/s10562-017-2138-x>
- Madhavan Nampoothiri, K., Nair, N. R., & John, R. P. (2010). An overview of the

- recent developments in polylactide (PLA) research. *Bioresource Technology*, *101*(22), 8493–8501. <https://doi.org/10.1016/j.biortech.2010.05.092>
- Masaki, K., Kamini, N. R., Ikeda, H., & Iefuji, H. (2005). Cutinase-Like Enzyme from the Yeast *Cryptococcus* sp . Strain S-2 Hydrolyzes Polylactic Acid and Other Biodegradable Plastics. *Applied and Environmental Microbiology*, *71*(11), 7548–7550. <https://doi.org/10.1128/AEM.71.11.7548>
- McKeown, P., & Jones, M. D. (2020). The Chemical Recycling of PLA: A Review. *Sustainable Chemistry*, *1*(1), 1–22. <https://doi.org/10.3390/suschem1010001>
- Mcneill, I. C., & Leiper, H. A. (1985a). Degradation Studies of Some Polyesters and Polycarbonates--2 . Polylactide : Degradation Under Isothermal Conditions , Thermal Degradation Mechanism and Photolysis of the Polymer. *Polymer Degradation and Stability*, *11*(4), 309–326. [https://doi.org/https://doi.org/10.1016/0141-3910\(85\)90035-7](https://doi.org/https://doi.org/10.1016/0141-3910(85)90035-7)
- Mcneill, I. C., & Leiper, H. A. (1985b). Degradation Studies of Some Polyesters and Polycarbonates 1 . Polylactide : General Features of the Degradation Under Programmed Heating Conditions. *Polymer Degradation and Stability*, *11*(3), 267–285. [https://doi.org/https://doi.org/10.1016/0141-3910\(85\)90050-3](https://doi.org/https://doi.org/10.1016/0141-3910(85)90050-3)
- Muniyasamy, S., Ofosu, O., John, M. J., & Anandjiwala, R. D. (2016). Mineralization of Poly (lactic acid) (PLA), Poly (3-hydroxybutyrate-co-valerate) (PHBV) and PLA / PHBV Blend in Compost and Soil Environments. *Journal of Renewable Materials*, *4*(2), 133–145. <https://doi.org/10.7569/JRM.2016.634104>
- Nishida, H. (2010). Thermal Degradation. In R. Auras, L. Lim, S. E. Selke, & H. Tsuji (Eds.), *Poly(Lactic Acid): Synthesis, Structures, Properties, Processing, and Applications* (pp. 401–412). Wiley. <https://doi.org/10.1002/9780470649848.ch23>
- Nishida, H., Mori, T., Hoshihara, S., Fan, Y., Shirai, Y., & Endo, T. (2003). Effect of tin on poly(L-lactic acid) pyrolysis. *Polymer Degradation and Stability*, *81*(3), 515–523. [https://doi.org/10.1016/S0141-3910\(03\)00152-6](https://doi.org/10.1016/S0141-3910(03)00152-6)

- NIST. (2020). *Isothermal Properties for Carbon dioxide*. National Institute of Standards and Technology (NIST-USA). https://webbook.nist.gov/cgi/fluid.cgi?Action=Load&ID=C124389&Type=IsoTherm&Digits=5&PLow=0&PHigh=300&PInc=5&T=313.15&RefState=DEF&TUnit=K&PUnit=bar&DUnit=mol%2Fm3&HUnit=kJ%2Fkg&WUnit=m%2Fs&VisUnit=uPa*s&STUnit=N%2Fm
- Noda, M., & Okuyama, H. (1999). Thermal catalytic depolymerization of poly(L-lactic acid) oligomer into LL-lactide : Effects of Al, Ti, Zn and Zr compounds as catalysts. *Chemical and Pharmaceutical Bulletin*, 47, 467–471. <https://doi.org/10.1248/CPB.47.467>
- Payne, J., McKeown, P., & Jones, M. D. (2019). A circular economy approach to plastic waste. *Polymer Degradation and Stability*, 165, 170–181. <https://doi.org/10.1016/j.polymdegradstab.2019.05.014>
- Pereda, S., Bottini, S. B., & Brignole, E. A. (2005). Supercritical fluids and phase behavior in heterogeneous gas-liquid catalytic reactions. *Applied Catalysis A: General*, 281(1–2), 129–137. <https://doi.org/10.1016/j.apcata.2004.11.019>
- Piemonte, V., & Gironi, F. (2013). Lactic Acid Production by Hydrolysis of Poly(Lactic Acid) in Aqueous Solutions: An Experimental and Kinetic Study. *Journal of Polymers and the Environment*, 21(1), 275–279. <https://doi.org/10.1007/s10924-012-0468-8>
- Pranamuda, H., Tokiwa, Y., & Tanaka, H. (1997). Polylactide degradation by an *Amycolatopsis* sp. *Applied and Environmental Microbiology*, 63(4), 1637–1640. <https://doi.org/10.1128/aem.63.4.1637-1640.1997>
- Qi, X., Ren, Y., & Wang, X. (2017). New advances in the biodegradation of Poly(lactic) acid. *International Biodeterioration and Biodegradation*, 117, 215–223. <https://doi.org/10.1016/j.ibiod.2017.01.010>
- Qureshi, M. S., Oasmaa, A., Pihkola, H., Deviatkin, I., Tenhunen, A., Mannila, J., Minkkinen, H., Pohjakallio, M., & Laine-ylijoki, J. (2020). Pyrolysis of plastic waste : Opportunities and challenges. *Journal of Analytical and Applied*

- Pyrolysis*, 152, 104804. <https://doi.org/10.1016/j.jaap.2020.104804>
- Sivri, S., Dilek Hacıhabiboğlu, Ç., & Sezgi, N. A. (2019). Synthesis and characterization of aluminum containing silica aerogel catalysts for degradation of PLA. *International Journal of Chemical Reactor Engineering*, 17(5), 1–10. <https://doi.org/10.1515/ijcre-2018-0163>
- Sivri, S., Dilek Hacıhabioğlu, Ç., & Sezgi, N. A. (2020). *High Yield, Eco-Friendly Recycling Method of Polylactic Acid Using Supercritical or Dense Gas Carbon Dioxide* (Patent No. WO2020263201).
- Song, X., Wang, H., Yang, X., Liu, F., Yu, S., & Liu, S. (2014). Hydrolysis of poly(lactic acid) into calcium lactate using ionic liquid [Bmim][OAc] for chemical recycling. *Polymer Degradation and Stability*, 110, 65–70. <https://doi.org/10.1016/j.polymdegradstab.2014.08.020>
- Song, X., Wang, H., Zheng, X., Liu, F., & Yu, S. (2014). Methanolysis of poly(lactic acid) using acidic functionalized ionic liquids as catalysts. *Journal of Applied Polymer Science*, 131(19), 1–6. <https://doi.org/10.1002/app.40817>
- Song, X., Zhang, X., Wang, H., Liu, F., Yu, S., & Liu, S. (2013). Methanolysis of poly(lactic acid) (PLA) catalyzed by ionic liquids. *Polymer Degradation and Stability*, 98(12), 2760–2764. <https://doi.org/10.1016/j.polymdegradstab.2013.10.012>
- Subramaniam, B. (2001). Enhancing the stability of porous catalysts with supercritical reaction media. *Applied Catalysis A: General*, 212(1–2), 199–213. [https://doi.org/10.1016/S0926-860X\(00\)00848-6](https://doi.org/10.1016/S0926-860X(00)00848-6)
- Tokiwa, Y., & Calabia, B. P. (2006). Biodegradability and biodegradation of poly (lactide). *Applied Microbiology and Biotechnology*, 72, 244–251. <https://doi.org/10.1007/s00253-006-0488-1>
- Tomita, K., Nakajima, T., Kikuchi, Y., & Miwa, N. (2004). Degradation of poly (L -lactic acid) by a newly isolated thermophile. *Polymer Degradation and Stability*, 84(3), 433–438.

<https://doi.org/10.1016/j.polymdegradstab.2003.12.006>

- Tsuji, H., Daimon, H., & Fujie, K. (2003). A new strategy for recycling and preparation of poly(L-lactic acid): Hydrolysis in the melt. *Biomacromolecules*, 4(3), 835–840. <https://doi.org/10.1021/bm034060j>
- Wang, W., Rao, L., Wu, X., Wang, Y., Zhao, L., & Liao, X. (2021). Supercritical Carbon Dioxide Applications in Food Processing. *Food Engineering Reviews*, 13(3), 570–591. <https://doi.org/10.1007/s12393-020-09270-9>
- Wang, X., Huang, Z., Wei, M., Lu, T., Nong, D., Zhao, J., Gao, X., & Teng, L. (2019). Catalytic effect of nanosized ZnO and TiO₂ on thermal degradation of poly (lactic acid) and isoconversional kinetic analysis. *Thermochimica Acta*, 672, 14–24. <https://doi.org/10.1016/j.tca.2018.12.008>
- Zhang, X., Heinonen, S., & Levänen, E. (2014). Applications of supercritical carbon dioxide in materials processing and synthesis. *RSC Advances*, 4(105), 61137–61152. <https://doi.org/10.1039/c4ra10662h>
- Zou, H., Yi, C., Wang, L., Liu, H., & Xu, W. (2009). Thermal degradation of poly (lactic acid) measured by thermogravimetry coupled to Fourier transform infrared spectroscopy. *Journal of Thermal Analysis and Calorimetry*, 97(3), 929–935. <https://doi.org/10.1007/s10973-009-0121-5>

APPENDICES

A. Solubility Calculations of Lactide in SCCO₂

Extraction temperature and pressure are taken into consideration to determine the lactide solubility. For this purpose, density values of CO₂ is found and given in Table A.1.

Table A.1 CO₂ density at given temperature and pressure

Pressure, bar	Temperature, °C	CO ₂ density, mol/L (NIST, 2020)
241	40	19.86
310	40	20.81
310	60	19.23
310	80	17.18

CO₂ mol is found using density and reactor volume;

$n_{CO_2} = \rho_{CO_2} * V_{reactor}$ where the reactor volume is 50 ml neglecting the volume occupied by PLA.

Lactide mol is found by following equation based on assumption that all products after PLA degradation are lactide.

$$n_{lactide} = \frac{m_{total\ product}}{M_{w_{lactide}}}$$

Mol fraction of lactide is calculated by;

$$x_{lactide} = \frac{n_{lactide}}{n_{lactide} + n_{CO_2}}$$

Mol fractions of lactide calculated at different temperatures and pressures are given in Table A.2.

Table A.2 Lactide mol fraction in CO₂ and lactide mixture

Pressure, bar	Temperature, °C	$n_{lactide}$, mol	n_{CO_2}, mol	$x_{lactide}$
241	40	0.005	0.9930	0.0050
310	40	0.005	1.0405	0.0048
310	60	0.005	0.9615	0.0052
310	80	0.005	0.859	0.0058

Literature solubility data of lactide and the required pressure to solve lactide completely at the extraction temperatures are found in the literature (Gregorowicz, 2008). A comparison of calculated solubility and solubility data from the literature is given in Table A.3.

Table A.3 Comparison of lactide mol fraction and required pressure with literature data at given temperature conditions

Temperature (experimental), °C	Pressure (experimental), bar	$x_{lactide}$	$x_{lactide}$ (literature)	Pressure (literature), bar
40	241	0.0050	0.0048	120
40	310	0.0048	0.0048	120
60	310	0.0052	0.0160	220
80	310	0.0058	0.0300	310

From Table A.3, it can be concluded that selected experimental pressures are enough to solve all of the lactides. Therefore, experiments are conducted with these data.

B. GC Calibration Factors

The retention time and response factor information of condensable products are determined by our research group and presented in Table B.1.

Table B.1 The retention times and response factors of the condensable products.

Compound	Retention Time (min)	Response Factor (RF)
Acetone	6.8	1
Lactic Acid	8.3	0.36
Meso - Lactide	14.2	1.41
D, L - Lactide	15.3	1.41

The mole of the condensable product is calculated using the following equation:

$$n_i = \frac{(Area)_i * RF_{acetone} * n_{acetone}}{(Area)_{acetone} * RF_i} \quad \text{Eqn. B1}$$

The mass of the condensable product is found by the equation below:

$$m_i = n_i * Mw_i \quad \text{Eqn. B2}$$

The retention time information for unknown products is given in Table B.2.

Table B.2 The retention time for unknown products

Unknown	Retention Time (min)
UK1	12.06
UK2	22.22
UK3	11.27
UK4	14.83
UK5	13.32
UK6	10.60
UK7	11.50

C. Equations for Yield Calculation

Calculation of yields for gas and solid is given in Eqn C1 and Eqn C2, respectively. Calculations are based on extracted product amount in the condenser, the product amount that remained in the reactor, and the initial PLA amount.

$$Yield_{solid} = \frac{W_{condenser} + W_{reactor}}{W_{PLA,initial}} * 100 \quad \text{Eqn. C1}$$

$$Yield_{gas} = \frac{(W_{PLA,initial} - W_{condenser} - W_{reactor})}{W_{PLA,initial}} * 100 \quad \text{Eqn. C2}$$

where $W_{PLA,initial}$ represents the initial PLA weight introduced in the reactor, $W_{condenser}$ is the extracted product weight obtained in the condenser, and $W_{reactor}$ is the product weight that remained in the reactor or in other words, the unextracted product.

Calculations for extraction and reactor yield are given in Eqn. C3 and Eqn. C4, respectively. These calculations are based on the extracted product amount in the condenser, the product amount that remained in the reactor, and the amount of coke formed during the reaction.

$$Yield_{extraction} = \left(\frac{W_{condenser}}{W_{condenser} + W_{reactor} - W_{coke}} \right) * 100 \quad \text{Eqn. C3}$$

$$Yield_{reactor} = \left(\frac{W_{reactor} - W_{coke}}{W_{condenser} + W_{reactor} - W_{coke}} \right) * 100 \quad \text{Eqn. C4}$$

$W_{condenser}$, $W_{reactor}$, and W_{coke} represents the extracted product weight obtained in the condenser, product weight that remained in the reactor, and weight of coke that appeared during the reaction, respectively.

Sample calculation for extraction experiment conducted at 80 °C, 310 bar for 60 min static extraction time;

$$W_{condenser} = 411 \text{ mg}$$

$$W_{reactor} = 170 \text{ mg}$$

$$W_{\text{coke}} = 84 \text{ mg}$$

$$W_{\text{PLA,initial}} = 1032 \text{ mg}$$

$$\text{Yield}_{\text{solid}} = \frac{411 \text{ mg} + 170 \text{ mg}}{1032 \text{ mg}} * 100 = 56\%$$

$$\text{Yield}_{\text{gas}} = \frac{(1032 \text{ mg} - 411 \text{ mg} - 170 \text{ mg})}{1032 \text{ mg}} * 100 = 44\%$$

$$\text{Yield}_{\text{extraction}} = \left(\frac{411 \text{ mg}}{411 \text{ mg} + 170 \text{ mg} - 84 \text{ mg}} \right) * 100 = 83 \%$$

$$\text{Yield}_{\text{reactor}} = \left(\frac{170 \text{ mg} - 84 \text{ mg}}{411 \text{ mg} + 170 \text{ mg} - 84 \text{ mg}} \right) * 100 = 17\%$$